Hindawi
Advances in Civil Engineering
Volume 2022, Article ID 2576122, 24 pages
https://doi.org/10.1155/2022/2576122

Research Article

Research on Numerical Simulation of Top-Down Construction Effect of Diaphragm Wall of Deep and Large Foundation Pit under Different Working Conditions in Complex Stratum

Fuxue Sun,[1] **Mingqing Liu**,[2] **Yunhui Zhu**,[2] **Xiaochun Li**,[3] **and Gang Ge**[3]

[1]*Wenzhou University, Wenzhou 325035, China*
[2]*Wenzhou University of Technology, Wenzhou 325035, China*
[3]*Shanghai Tunnel Engineering Co., Ltd, Shanghai 200000, China*

Correspondence should be addressed to Mingqing Liu; 846765019@qq.com

Received 17 July 2021; Revised 6 January 2022; Accepted 5 March 2022; Published 11 April 2022

Academic Editor: Milos Knezevic

In order to study the construction effect of deep and large foundation pit excavation and its impact on the surrounding environment under complex stratum conditions, the deep and large foundation pit of the top-down construction method of shield exit shaft of S2 line of Wenzhou City railway is taken as the research object in this paper. According to the complex geological conditions of deep soft soil layer with underlying inclined rock surface in Wenzhou, the numerical simulation method is used to carry out the related research. The simulation results of the deformation characteristics of the diaphragm wall under two different working conditions which are the same length diaphragm wall and the suspended foot diaphragm wall are compared and analyzed. According to the analysis results, the suspended foot diaphragm wall is determined as the final construction scheme of the diaphragm wall, and it is verified by field measurement. The research results can provide technical support for the construction of similar projects. At the same time, it can also provide basic accumulation for the construction of major projects in Wenzhou.

1. Introduction

With the construction of the urban underground track, a large number of foundation pit projects appear. Foundation pit engineering is a multidisciplinary system engineering involving structural engineering, engineering mechanics, soil mechanics, foundation engineering, engineering monitoring technology, and construction organization management. It is a complex technology with two branches of civil engineering, which are architectural engineering and geotechnical engineering [1]. Generally, the regional geological conditions of foundation pit engineering are relatively poor, generally weak, or weak soil layers, and the occurrence and change forms of groundwater are diverse, such as the southeast coast of China. In this case, the key links of foundation pit engineering construction, including excavation, support, and dewatering, are often complex, which is a highly risky and challenging topic in the field of geotechnical engineering [2]. The traditional excavation method of foundation pit is sloping excavation; that is, large open excavation without support structure or vertical excavation after certain support measures (such as anchor support, retaining wall support, and pile wall support) is adopted. After reaching the predetermined excavation depth, the concrete bottom plate is poured, and then the construction method is from bottom to top, or a combination of the two, and the sloping excavation is adopted for the upper part, the lower part adopts the construction method of support and excavation [3]. Although the above excavation methods are simple and fast, they have high requirements for engineering geological conditions, hydrogeological conditions, sloping excavation space, and excavation depth and are not suitable for the construction of underground space in large cities with poor hydrogeological conditions and dense populations. Under this background, the top-down construction method of the foundation pit

came into being. Its important feature is how to deal with the sliding resistance, horizontal resistance, and vertical load capacity of the basement structure. The common method to transfer the vertical load to the foundation is to use the frame column or Qiao. At this time, the outer wall of the basement can be served by the diaphragm wall. Italy is the first country in the world to have the reverse practice, and then, it has gradually developed in western developed countries such as the United States and Japan. So far, many engineering practices show that the top-down construction method of foundation pit is an effective construction method for multistorey underground space structures of buildings and roads in big cities [4,5].

So far, the pace of theoretical research on the top-down construction method is relatively slow, showing the phenomenon that theoretical research lags behind engineering practice [6–10]. There are three main research methods: (1) using many engineering practices and the basic theory of soil mechanics to summarize the engineering experience and practical methods, (2) using engineering monitoring technology and field test to capture the information of monitoring points during construction, and (3) the finite element simulation of the project carried out by using computer technology. The research contents mainly include the following: research on water and soil pressure and deformation around foundation pit; research on stress, strain, and displacement of foundation pit support structure; and study on the settlement difference between intermediate pile (column) and diaphragm wall.

In the study of soil displacement, Hsieh and Ou [11] fitted and analyzed 9 foundation pit engineering examples with different support methods of top-down construction method and down-top construction method and considered that the conclusion of soil deformation law caused by down-top construction method can be applied to the top-down construction method. Yoo and Lee [12] used the hardening soil constitutive model to establish a two-dimensional numerical model to study the characteristics of surface soil displacement. In the study of internal force and deformation of foundation pit retaining structure, Bose and Som [13] used numerical simulation to study the influence of diaphragm wall height, excavation width, and support structure prestress on foundation pit excavation; Ng et al. [14] used the Cambridge model to study the excavation process and results of multisupport foundation pit in cohesive soil, compared with the actual project, and obtained some meaningful conclusions; Finno et al. [15] studied the influence of foundation pit excavation on soil deformation and the influence of foundation pit support structure on pore water pressure by means of a test. The focus or foundation of the research on the differential settlement of top-down construction method lies in the research on pile foundation settlement theory. Poulos has made outstanding contributions in this regard. The Poulos elastic theory model established by Poulos has been used for reference by many scholars [16]. Because the elastic theory method assumes that the soil layer is uniform and the stiffness is constant, it can not reflect the anisotropy and stratification characteristics of the actual foundation soil. On this basis, scholars at home and abroad introduce correction factors to modify and supplement Poulos's elastic theory model in varying degrees according to the actual formation conditions.

In addition, as an important retaining structure of the foundation pit, the diaphragm wall has the advantages of good overall, large stiffness, and convenient construction. It is still loved by builders. Bolton and Powrie [17] described the construction and foundation pit design mechanism by using an indoor centrifuge test and studied the behavior of diaphragm wall before foundation pit instability, including surface settlement outside the foundation pit and bending moment of the diaphragm wall. Ou et al. [18] conducted field measurement on the foundation pit excavated by the top-down construction method, analyzed the data, and concluded that the horizontal displacement of soil close to the diaphragm wall is similar to that of the wall. Graham [19] simulated and studied the deformation of diaphragm walls during foundation pit construction and analyzed the law of wall displacement and internal force. Wang et al. [20] analyzed a large number of field-measured data of ground connecting wall deformation in foundation pit and pointed out that the deformation of ground connecting wall in top-down construction method is smaller than that in the forward method. Xu et al. [21] analyzed the deformation law of diaphragm walls in different foundation pit projects by studying a large number of practical projects using diaphragm walls as a support structure in the deep foundation pit in Shanghai. Qiu et al. [22] established a practical engineering numerical model through the finite element numerical simulation research method to simulate the excavation process of the foundation pit and found that the greater the excavation depth of the foundation pit, the greater the deformation of the diaphragm wall.

To sum up, although the construction technology and relevant theories of the top-down construction method have achieved certain results and the application has been popularized, it is still applied as a special construction method, which is mainly used when there are special requirements for the project, or when the traditional method can not meet the requirements and is very uneconomic. At the same time, the combined action of the diaphragm wall and top-down construction method can reduce the deformation of the foundation pit. The deformation law of the diaphragm wall provides guidance for subsequent foundation pit design and construction and ensures the safety of foundation pit construction. In this paper, based on the top-down construction method of deep foundation pit for shield exit shaft of S2 line of Wenzhou City railway, aiming at the complex geological conditions of deep soft soil layer with underlying inclined rock surface in Wenzhou, the deformation characteristics of different diaphragm walls (diaphragm wall with the same length and suspended foot diaphragm wall) are compared and analyzed by using numerical simulation method, and the suitable construction scheme of diaphragm wall is determined, It can provide a reference for foundation pit engineering under similar geological conditions.

2. Project Overview

The project is located at the mouth of Oujiang River, connecting Qitoushan, Huanghua Town, Yueqing City, and Lingkun Town, Longwan District. It is an important part of line S2 of the Wenzhou City railway. The shield tunneling method is used for construction. The tunnel location is shown in Figure 1. Jiangbei's working shaft is the exit shaft of the shield tunnel, and foundation pit engineering is an important construction item of the Oujiang North portal tunnel. The length of the foundation pit is 43 m, the width is 21.9 m or 27.6 m, the excavation depth is 51.63 m (as shown in Figure 2), and the excavation depth is 51.63 m. Jiangbei working well is located in the deep muddy soil layer of the Oujiang shoal area. The upper part is the muddy soil and clay layer, and its thickness is about 46 m. There is a deep riprap layer in the middle and a weakly weathered tuff layer in the lower part. The rock surface is horizontally extroverted, and the geological conditions are complex (as shown in Figure 3). The foundation pit is protected by diaphragm wall, the thickness of the diaphragm wall is 1.5 m, the width of the standard section is generally 5.5 m, the length of the local special-shaped diaphragm wall is adjusted appropriately (as shown in Figure 4), and the reinforced concrete ring frame beam and each floor plate are used as support (as shown in Figure 5).

To sum up, the deep foundation pit engineering of Jiangbei working well is the deepest foundation pit in Zhejiang Province, and it faces multiple complex geology. Therefore, how to carry out diaphragm wall construction and foundation pit excavation and support under complex geological conditions and effectively control the deformation of foundation pit to ensure construction safety has become a construction difficulty of this project, which is also the research focus of this paper. In this paper, the numerical simulation method is used to compare and analyze the construction effect of the top-down method of diaphragm wall foundation pit under different working conditions and, finally, determine the best design scheme of diaphragm wall construction and foundation pit excavation and support suitable for the project.

3. Research on Numerical Simulation

Midas GTS software is used in numerical simulation, which can carry out two-dimensional and three-dimensional finite element numerical modeling for geotechnical engineering and analyze the stress and deformation of structural components and soil materials in engineering. The simulation results are very similar to the measured data.

3.1. Numerical Model

3.1.1. Model Size. According to the actual size of the foundation pit, the calculation model diagram is established, as shown in Figure 3. The length of the foundation pit relying on the project is 43 m, the left width is 21.9 m, the right width is 27.6 m, and the excavation depth is 51.63 m. According to the previous modeling experience, the size of the foundation pit model can generally be 3–5 times the excavation depth of the foundation pit [23]. Finally, the overall size of the foundation pit model is determined as the length is 287 m, the width is 227.6 m, and the height is 100 m.

FIGURE 1: Schematic diagram of the location of Oujiang Beikou tunnel.

3.1.2. Formation Treatment Method. According to the detailed investigation report of the Oujiang North portal tunnel, the stratum is fine layered. Through sorting out and merging the soil materials with similar properties, the soil materials are divided into five different layers, and the modified Mohr-Coulomb constitutive model is adopted for the soil materials. The material parameters of each layer are shown in Table 1. (Note: the parameters that cannot be provided in the geological survey report are calculated by the empirical method. The other two stiffness properties can be selected according to the compression modulus of a certain ratio. Generally, the secant modulus is equal to the tangent modulus and three times the compression modulus.)

For the inclined rock surface, according to the geological survey data, the inclined rock surface is diagonally inclined, and the slope of the rock surface is not uniform. It is difficult to model and simulate according to the actual trend, and there are many irregular grid cells, which lead to poor quality of the grid and reduce the simulation speed. In order to meet the needs of simulation calculation, according to the depth of the rock surface around the foundation pit determined by the survey, after determining the depth of the weathered rock at the interface between the rock surface and the foundation pit, the rock surface trend inside the foundation pit is determined by the slope average method, and the rock surface trend outside the foundation pit is extended according to the slope inside the foundation pit to form the internal rock surface trend of the model. The size of the completed model is shown in Figure 6.

3.2. Selection of Structural Elements and Material Parameters. The supporting structure of the deep foundation pit in Beikou well is mainly the diaphragm wall, supporting plate, and reinforced concrete ring frame beam, as shown in Figure 5. The elastic constitutive model is selected for all supporting structures, in which the diaphragm wall and each floor structure adopt a two-dimensional plate element,

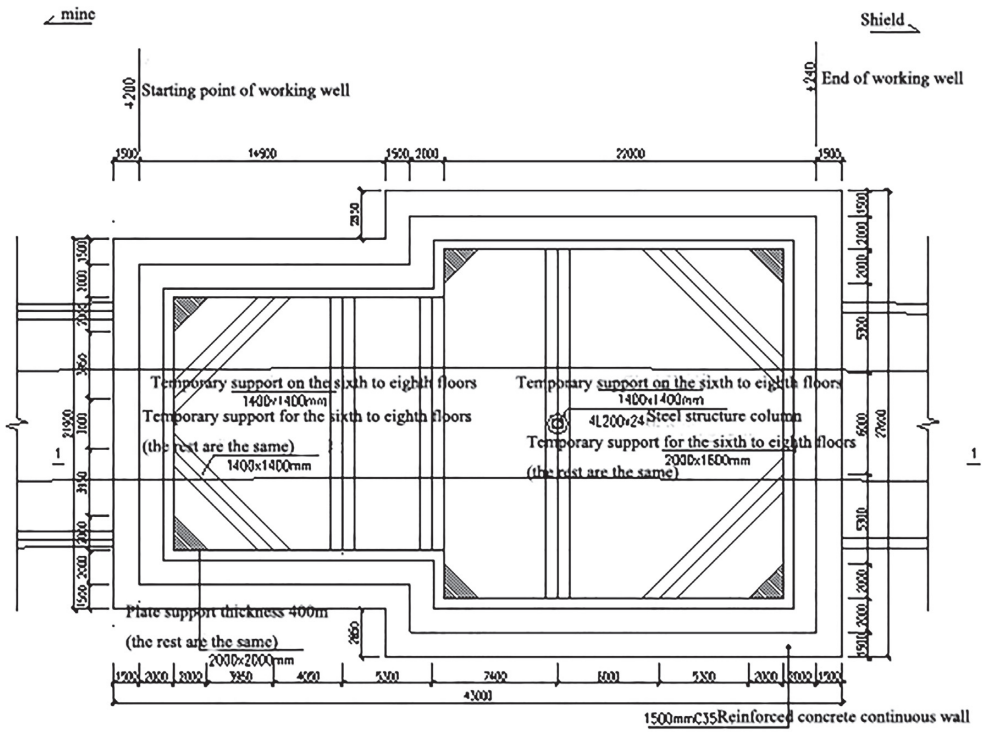

Figure 2: Layout map of Jiangbei working well.

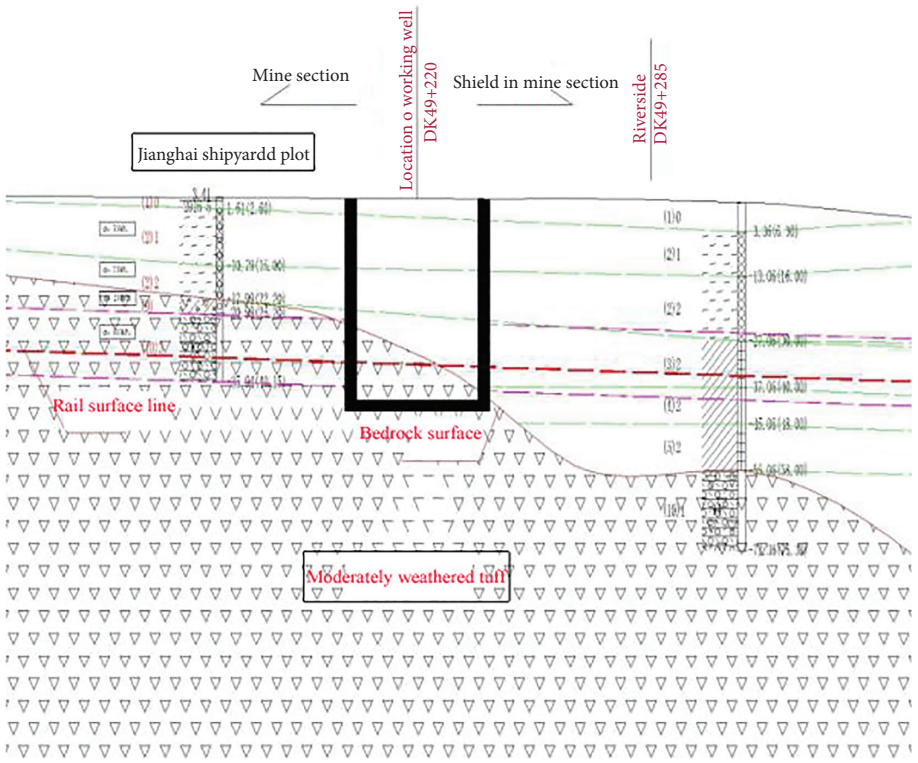

Figure 3: Geological profile of Jiangbei working well.

which is extracted from the three-dimensional solid element. The reinforced concrete ring frame beam is mainly flexural, and its length is larger than the cross-sectional area, so a one-dimensional beam element is adopted, which is extracted from the three-dimensional solid element. The material parameters of the supporting structure are shown in Table 2.

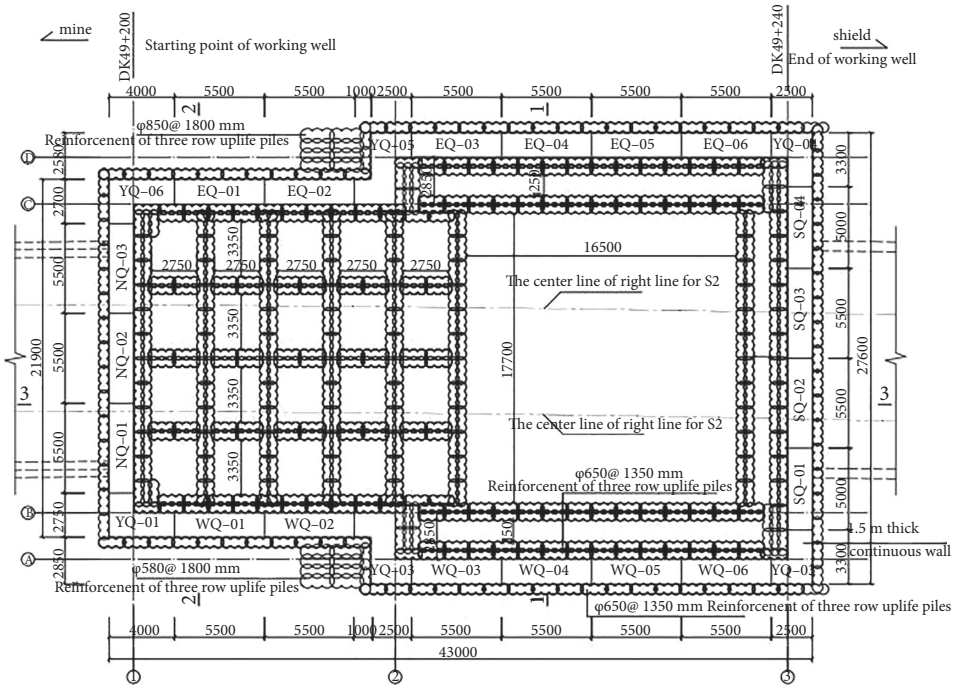

Figure 4: Division map of ground connecting wall in Jiangbei working well.

3.3. Boundary Conditions and Mesh Generation. In the length direction (X direction) of the model, the displacement of the X-axis is limited, that is, $u = 0$, $v \neq 0$, and $w \neq 0$. In the width direction (Y direction), the displacement of the Y-axis is limited, that is, $u \neq 0$, $v = 0$, and $w \neq 0$. In the height direction (z direction), the upper boundary of the model is free, i.e., unrestricted, and the lower boundary of the model is fully constrained, i.e., $u = 0$, $v = 0$, and $w = 0$ (U is the displacement in the X direction, V is displacement in the Y direction, and W is displacement in the Z direction). In this model, a hybrid grid is used.

3.4. Determination of Simulated Construction Process of Top-Down Method. The deep foundation pit is constructed by the top-down method. According to the design and construction technology of the foundation pit, the foundation pit excavation is simulated according to the actual technology. The foundation pit excavation is divided into 12 steps, and the specific construction process is shown in Table 3.

3.5. Determination of Simulation Conditions. According to the needs of the project, the following two comparative conditions are determined for research: ① the bottom of the diaphragm wall is at the same elevation and ② suspended foot diaphragm wall. The construction procedures of the two conditions are shown in Table 3. According to the needs of simulation, the horizontal displacement, bending moment deformation and surrounding ground settlement of diaphragm wall are selected as the construction effect indexes.

3.6. Calculation Assumption. In this paper, based on the foundation pit of the exit well of the project, the calculation model is established considering the surrounding soil. According to the actual stratum situation and the calculation needs of the model, the following assumptions are made. ① The soil is isotropic and evenly distributed, and the soil is isotropic and uniformly distributed. ② The influence of the surrounding environment induced by diaphragm wall construction is not considered. ③ The influence of soil drainage consolidation and groundwater seepage is not considered.

4. Numerical Simulation of Construction Effect of Diaphragm Wall Foundation Pit with Top-Down Method under Different Working Conditions

4.1. Numerical Simulation Study on Construction Effect of Top-Down Construction Method for Foundation Pit with Diaphragm Wall of the Same Length. The foundation pit construction is divided into 12 steps, and there are many excavation conditions. In the simulation, the first, third, fifth, seventh, and tenth excavation is selected (corresponding to the process number in Table 3 is third, fifth, seventh, ninth, and twelfth). These five excavation conditions are used to study and analyze the foundation pit construction effect.

4.1.1. Design of Diaphragm Wall with the Same Length. The excavation depth of the foundation pit is 51.63 m, which belongs to a super deep foundation pit with a weak stratum. The original design diaphragm wall of the foundation pit is

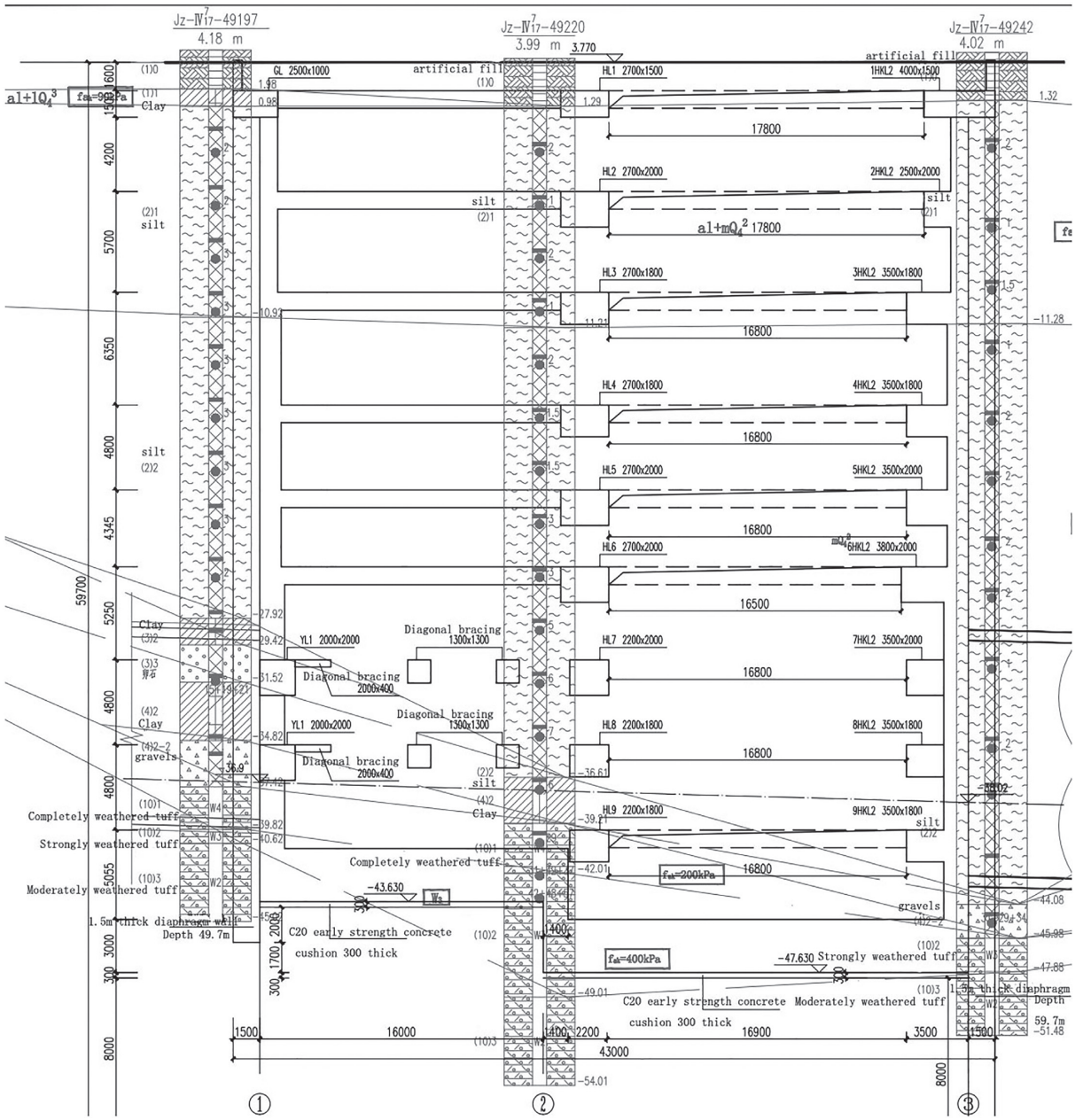

Figure 5: Section diagram of foundation pit supporting structure.

Table 1: Material parameters of soil layer.

Number	Layer	Layer thickness (m)	Compression modulus (MPa)	Poisson's ratio	Unit weight (kN/m^3)	Cohesion (kPa)	Internal friction angle (°)
①	Silt 1	18	1.97	0.30	18	6.05	2.93
②	Silt 2	14	2.09	0.30	15	6.38	3.11
③	Clay 1	14.8	2.98	0.40	20	10.23	3.10
④	Clay 2	3.18	3.80	0.35	18	12.45	7.58
⑤	Tuff	1.65	500.00	0.30	23	20.00	33.00

the same length diaphragm wall. The diaphragm wall is made of C45 waterproof concrete, with the bottom at the same elevation, the depth of 59.80 m, and the thickness is 1.5 m, as shown in Figure 7.

4.1.2. Analysis of Horizontal Displacement Simulation Results of Diaphragm Wall with the Same Length. The horizontal displacement contour plot of the diaphragm wall with the same length under five excavation conditions is shown in

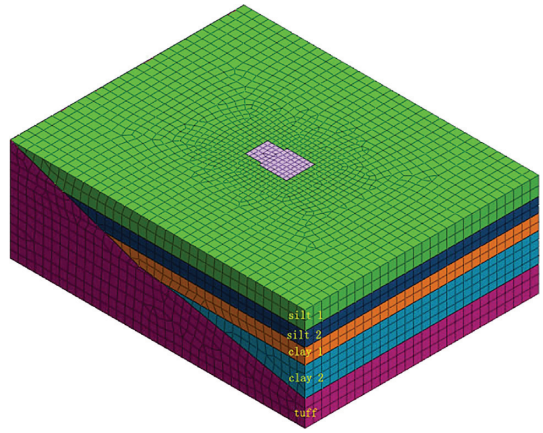

Figure 6: Overall calculation model of foundation pit.

Table 2: Material parameters of supporting structure.

Structure name	Element type	Constitutive model	Modulus of elasticity (kN/m^2)	Poisson's ratio	Unit weight (kN/m^3)	Thickness/diameter (m)
Diaphragm wall	Plate	Elastic	32500000	0.2	24.5	1.5
Ring frame beam	Beam	Elastic	32500000	0.2	24.5	3.5×1.8
Top plate/middle plate	Plate	Elastic	32500000	0.2	24.5	0.4
Floor	Plate	Elastic	32500000	0.2	24.5	3

Table 3: Details of construction procedures.

Process number	Process node
1	The original stratum is established, and the initial stress is analyzed by applying boundary constraint and self-weight load
2	Activate diaphragm wall and clear displacement
3	The first excavation to −2.000 m activates the first ring frame beam and roof
4	The second excavation was to −7.700 m, and the second ring frame beam and the middle slab of the negative first floor were activated
5	After the third excavation to −13.400 m, the third ring frame beam and the middle slab of the second floor were activated
6	The fourth excavation to −19.750 m, the fourth ring frame beam and the negative third floor slab were activated
7	The fifth excavation to −24.550 m, the fifth ring frame beam and the negative fourth floor slab were activated
8	The sixth excavation was to −28.895 m, and the sixth ring frame beam and the middle slab of the fifth floor were activated
9	The seventh excavation was carried out to −34.145 m, and the seventh ring frame beam and the middle slab of the sixth floor were activated
10	The eighth excavation to −38.945 m, the eighth ring frame beam and the negative seventh floor middle plate were activated
11	The ninth excavation was carried out to −43.575 m, and the ninth ring frame beam and the middle slab of the eighth floor were activated
12	The tenth excavation to −51.630 m, the floor was activated

Figure 8. In the contour plot, the one on the left is the west wall, and the one on the right is the east wall (the same below).

The horizontal displacement data of the diaphragm wall under five excavation conditions obtained from Figure 8 are sorted and analyzed, and the depth-displacement curve of the diaphragm wall can be obtained, as shown in Figure 9, and the maximum horizontal displacement and depth data of diaphragm wall can be summarized into a table, as shown in Table 4.

It can be seen from the above that the horizontal displacement of the diaphragm wall is small in the first excavation. With the excavation of the foundation pit, the pouring of intermediate plate structure, and the support of ring frame beam, the horizontal displacement curve of diaphragm wall forms the deformation law of "small at both ends, large in the middle." The maximum horizontal displacement of the east wall is larger than that of the west wall, which is due to the existence of an inclined rock surface, and the displacement and deformation laws of the east and west walls are basically the same. With the increase of the excavation depth of the foundation pit, the maximum horizontal displacement of the diaphragm wall increases continuously, and the position of the maximum

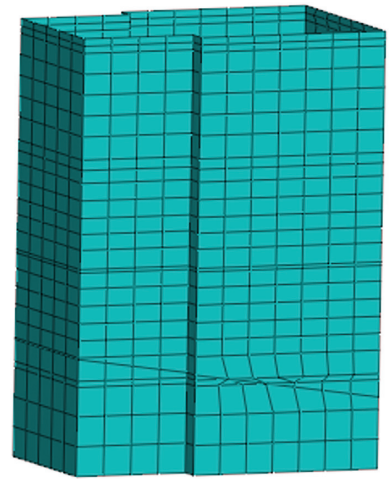

Figure 7: Schematic diagram of the bottom-level wall-to-wall model.

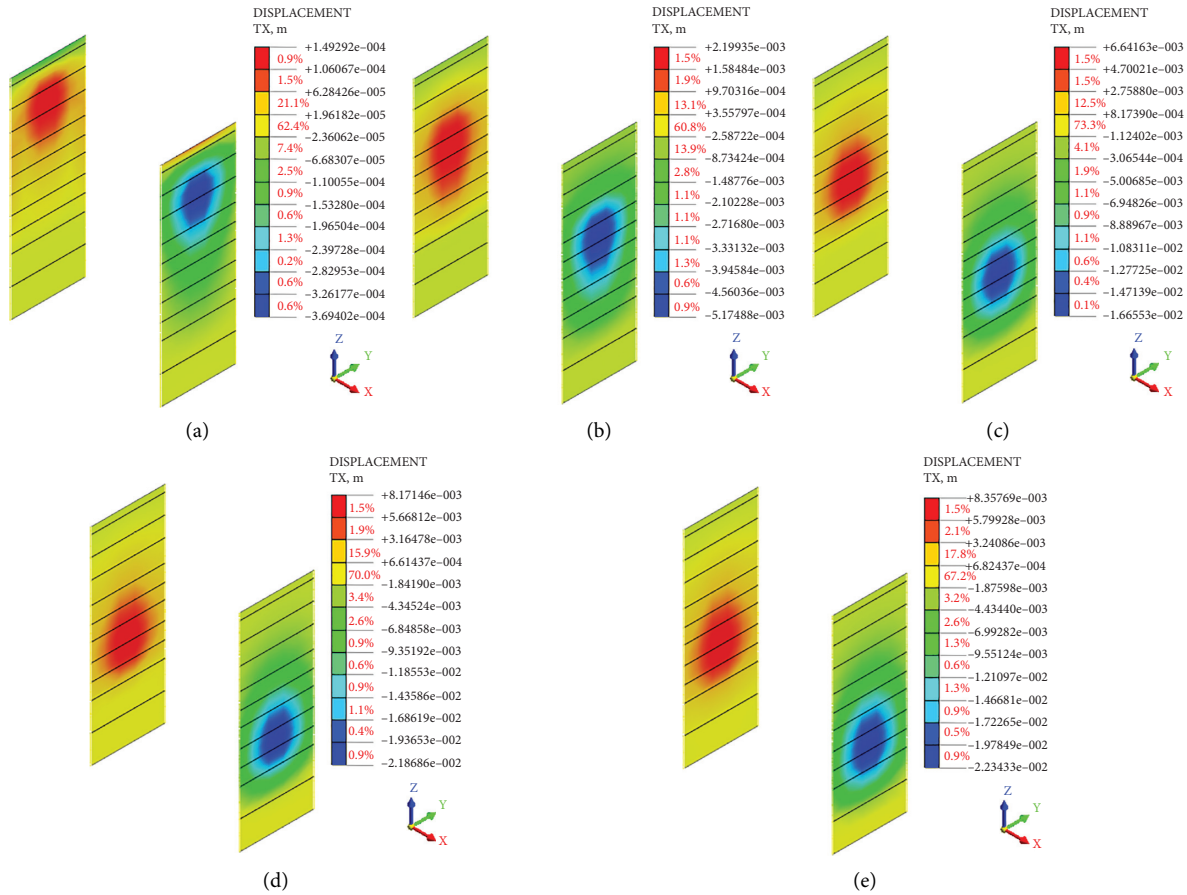

Figure 8: The horizontal displacement contour plot of the diaphragm wall with the same length under five excavation step conditions. (a) The first excavation step. (b) The third excavation step. (c) The fifth excavation step. (d) The seventh excavation step. (e) The tenth excavation step.

horizontal displacement moves downward. Due to the constraint of rock on the diaphragm wall, the final maximum horizontal displacement is above the excavation surface, and the maximum horizontal displacement is about 3/5~3/4 times of the final excavation depth of the foundation pit.

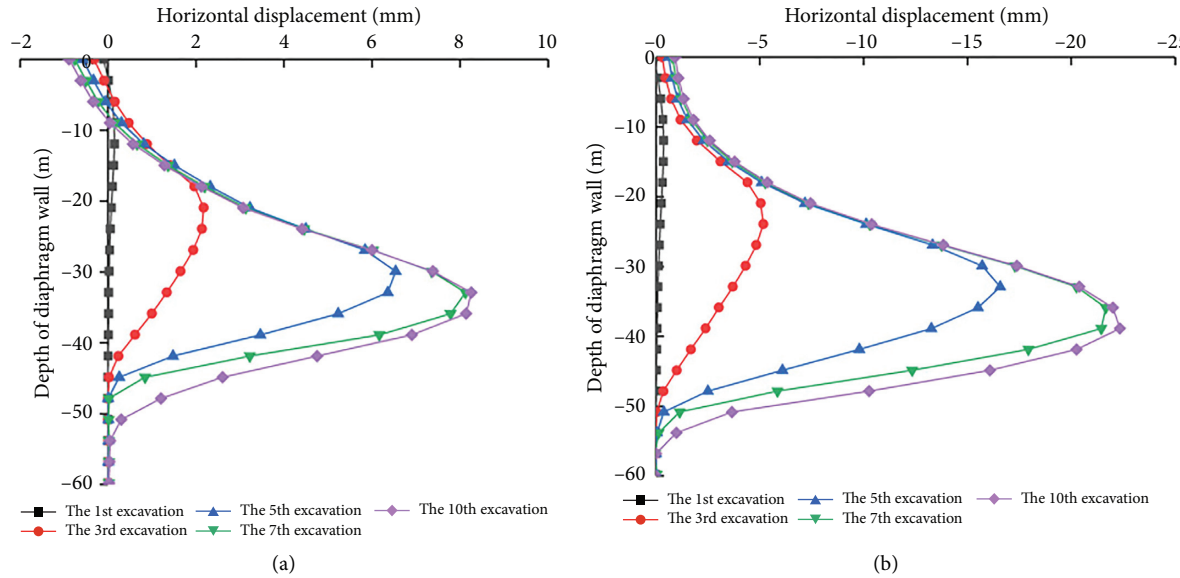

Figure 9: The horizontal displacement curve of the diaphragm wall. (a) West wall. (b) East wall.

Table 4: Summary of the corresponding depth of the maximum horizontal displacement of the ground connecting wall.

Working procedure	Diaphragm wall (west)		Diaphragm wall (east)	
	Maximum horizontal displacement (mm)	The depth of diaphragm wall (m)	Maximum horizontal displacement (mm)	The depth of diaphragm wall (m)
The first excavation step (−2.000 m)	0.145	−11.96	−0.364	−11.96
The third excavation step (−13.400 m)	2.171	−20.93	−5.171	−23.92
The fifth excavation step (−24.550 m)	6.537	−29.90	−16.581	−32.89
The seventh excavation step (−34.145 m)	8.126	−32.89	−21.666	−35.88
The tenth excavation step (−51.630 m)	8.256	−32.89	−22.341	−38.87

4.1.3. Analysis of the Bending Moment Simulation Results of Diaphragm Wall with the Same Length. The bending moment contour plot of the diaphragm wall under five excavation conditions is shown in Figure 10.

The depth-bending moment curve of the diaphragm wall can be obtained by sorting and analyzing the bending moment data of the diaphragm wall under five excavation step conditions, as shown in Figure 11, and the maximum bending moment and depth data of the diaphragm wall can be summarized into a table, as shown in Table 5.

It can be seen from the above that the bending moment of the diaphragm wall is small in the first excavation, and there is a reverse bending point. With the progress of excavation, the bending moment of the diaphragm wall increases gradually, and the bending moment in the final excavation stage decreases slightly compared with that in the previous stage. The maximum positive moment is larger than the maximum negative moment at each excavation stage. Due to the existence of inclined strata, the maximum bending moment of the east wall is larger than that of the west wall in each excavation stage, and the deformation law of the east wall and the west wall is basically the same, but asymmetric. With the increase of the excavation depth of the foundation pit, the maximum positive (negative) bending moment of the diaphragm wall increases continuously (except for the tenth excavation). During the tenth excavation, the maximum positive bending moment of the diaphragm wall decreases, the position of the maximum positive bending moment first moves down and then rises, the original position remains unchanged, and the position of the maximum negative bending moment does not change with the change of excavation stage. In each excavation stage, the maximum positive bending moment of the diaphragm wall is larger than the maximum negative bending moment. The maximum positive bending moment of the diaphragm wall is about 7/10~3/4 times of the final excavation depth of the foundation pit, and the maximum negative bending moment is about 4/5~49/50 times of the final excavation depth of the foundation pit.

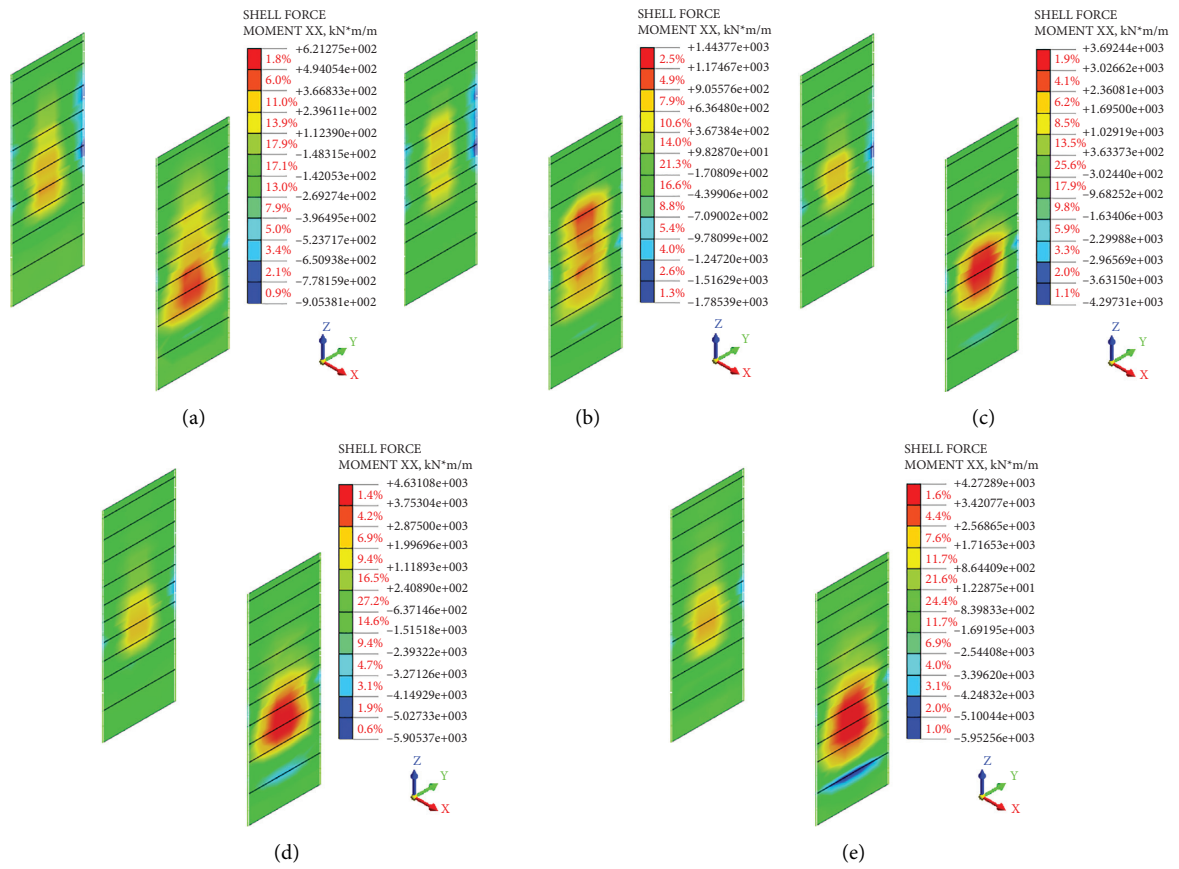

FIGURE 10: The bending moment contour plot of suspended diaphragm wall under five excavation step conditions. (a) The first excavation step. (b) The third excavation step. (c) The fifth excavation step. (d) The seventh excavation step. (e) The tenth excavation step.

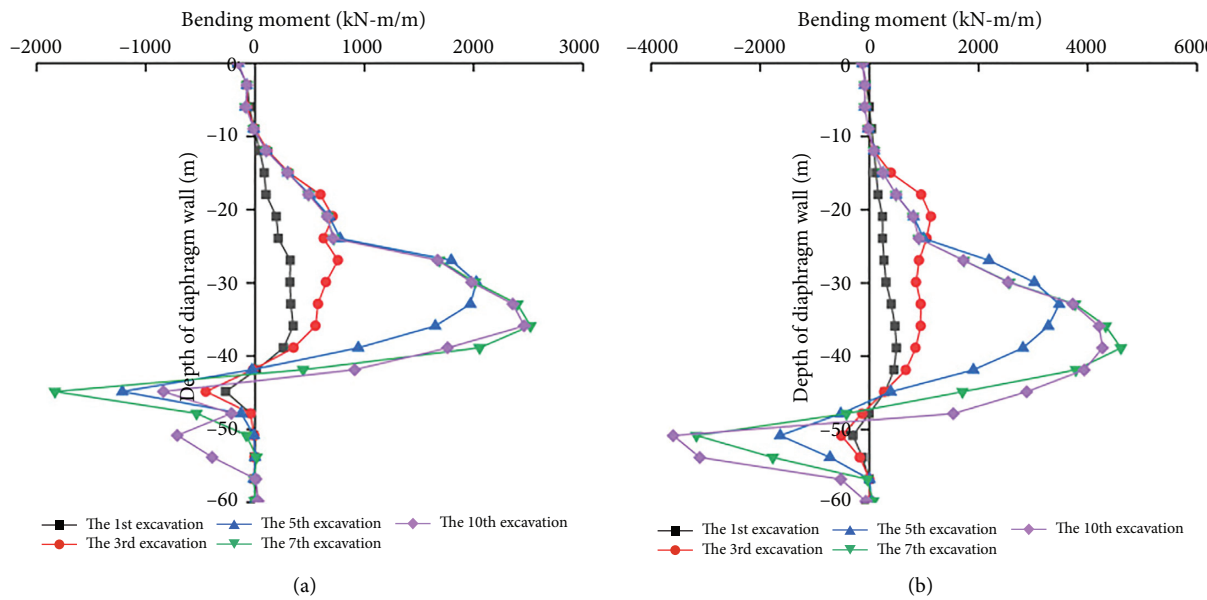

FIGURE 11: The bending moment curve of the diaphragm wall. (a) West wall. (b) East wall.

4.1.4. Analysis of Ground Settlement Simulation Results of Diaphragm Wall with the Same Length. The contour plot of soil surface settlement and deformation under five excavation conditions is shown in Figure 12.

By sorting and analyzing the simulated data of soil surface settlement under five excavation conditions, the surface settlement distance curve from the foundation pit can be obtained, as shown in Figure 13, and the data of the

Table 5: Summary of maximum bending moment corresponding to the depth of the ground wall.

Working procedure	Diaphragm wall (west)		Diaphragm wall (east)	
	Maximum bending moment (kN·m/m)	The depth of the diaphragm wall (m)	Maximum bending moment (kN·m/m)	The depth of the diaphragm wall (m)
The first excavation step (−2.000 m)	349.896/−269.976	−35.88/−44.85	497.000/−300.185	−38.87/−50.83
The third excavation step (−13.400 m)	757.587/−449.852	−26.91/−44.85	1127.313/−511.097	−20.93/−50.83
The fifth excavation step (−24.550 m)	2024.333/−1214.235	−29.90/−44.85	3480.993/−1632.490	−32.89/−50.83
The seventh excavation step (−34.145 m)	2518.406/−1831.024	−35.88/−44.85	4609.055/−3168.472	−38.87/−50.83
The tenth excavation step (−51.630 m)	2462.475/−838.087	−35.88/−44.85	4271.144/−3594.525	−38.87/−50.83
Remarks	Among the maximum bending moments in the table, the maximum positive bending moment value is before "/," and the maximum negative bending moment value is after "/," respectively, corresponding to the depth of the diaphragm wall			

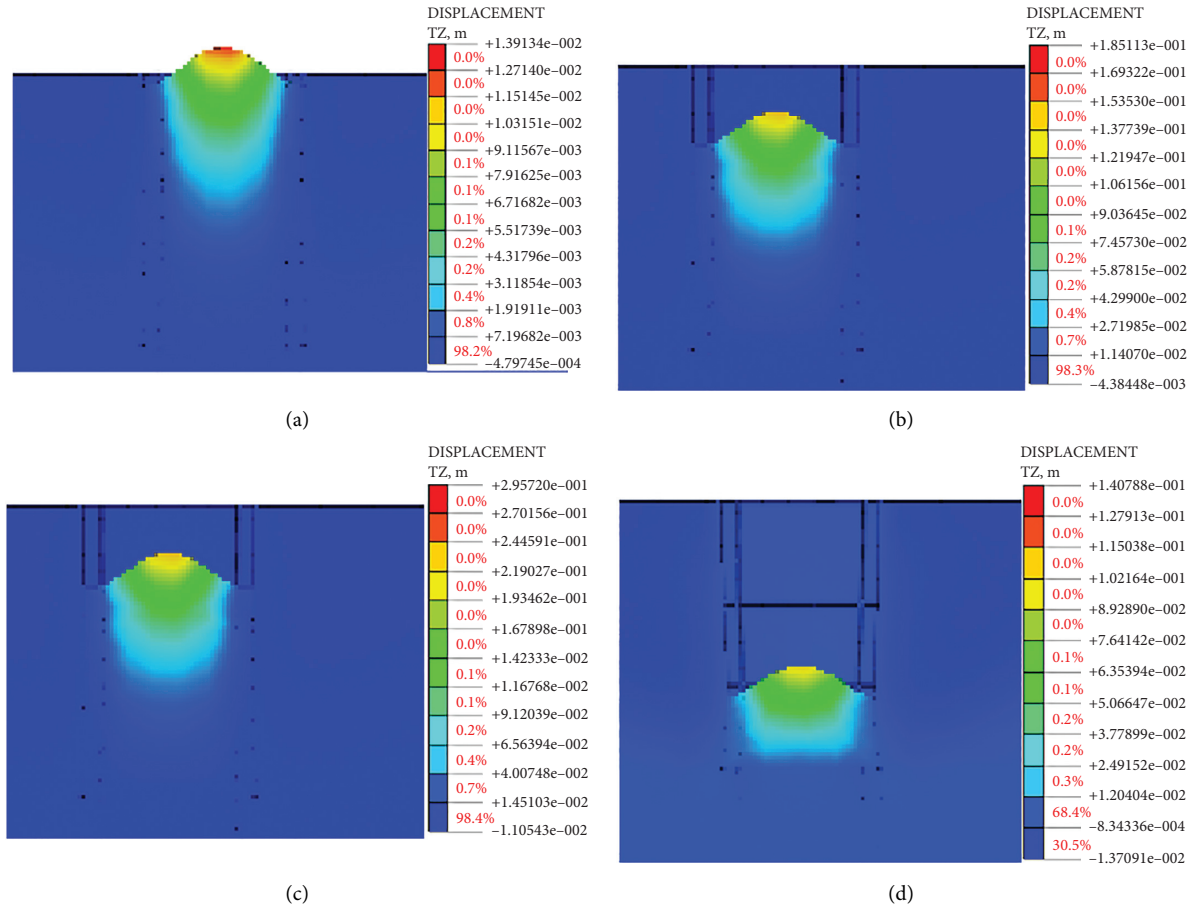

Figure 12: Continued.

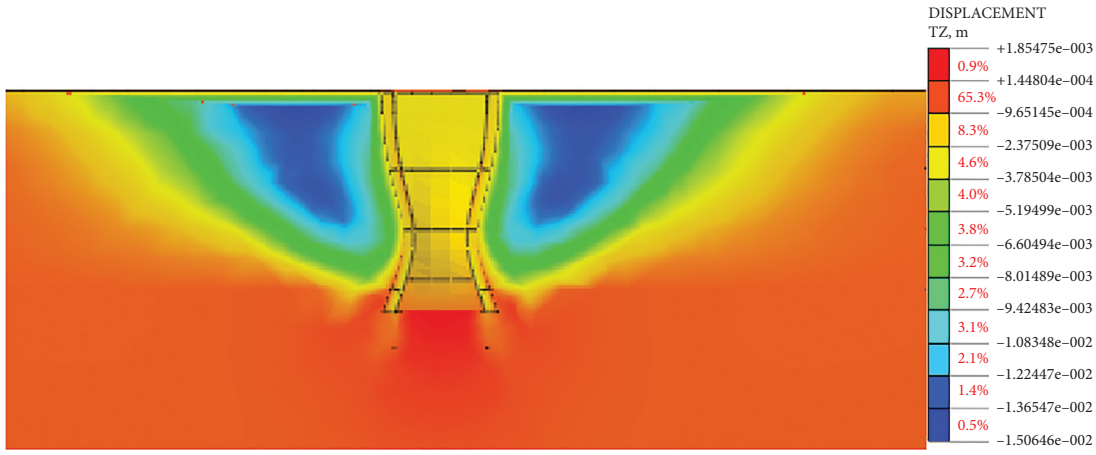

(e)

Figure 12: The contour plot of surface settlement and deformation under five excavation conditions. (a) The first excavation step. (b) The third excavation step. (c) The fifth excavation step. (d) The seventh excavation step. (e) The tenth excavation step.

location of the maximum surface settlement can be summarized into a table, as shown in Table 6.

Through comprehensive analysis of Figures 12 and 13 and Table 6, the following conclusions can be obtained:

(1) During the first excavation, the surface settlement of the soil is very small. The maximum surface settlement of the soil on the east and west sides is about 0.5 mm. The maximum settlement is located 10 m away from the edge of the foundation pit, and the settlement beyond 20 m is almost zero.

(2) During the third excavation, the soil surface settlement increased, and the maximum settlement was about 4.0~4.5 mm. The soil surface settlement position changed, all located 15 m away from the edge of the foundation pit, and the soil surface settlement outside 60 m was small.

(3) During the fifth excavation, the surface settlement of the soil continued to increase, and the maximum surface settlement was about 11.0 mm, an increase of about twice that of the third excavation, which was consistent with the sudden increase of the horizontal displacement and a bending moment of the diaphragm wall during the fifth excavation. Due to the deformation law of the diaphragm wall, the surface also had a large settlement. The maximum surface settlement position of the soil in the west remained unchanged, and it was still 15 m away from the foundation pit division. The maximum ground settlement position of the soil on the east side changes, which is 20 m away from the pit edge of the foundation pit, and the ground settlement of the soil outside 80 m is about 0.8 mm.

(4) During the seventh excavation, the surface settlement of soil continued to increase with a small increase. The maximum surface settlement of soil was about 13.0~14.0 mm, the maximum surface settlement position remained unchanged (15 m in the west and 20 m in the east), and the surface settlement outside 85 m was about 0.9 mm.

(5) During the tenth excavation, the soil surface settlement continued to increase with a smaller increase. The maximum soil surface settlement was about 15.0 mm, and the maximum surface settlement position remained unchanged (the west side is 15 m and the east side is 20 m). The maximum surface settlement is about 0.029% of the excavation depth of the foundation pit of 51.630 m, about 67% of the maximum horizontal displacement of the diaphragm wall. The maximum surface settlement is located 20 m away from the edge of the foundation pit, about 0.4 times the excavation depth of the foundation pit of 51.630 m.

(6) The maximum surface settlement of the soil in the east is slightly greater than that in the west (except for the third excavation step). The surface settlement curve of the soil in each construction stage first increases and then decreases with the distance from the edge of the foundation pit and finally tends to be stable, showing a "groove shape." According to the curve, the law of surface settlement and deformation on the east and west sides is basically the same. With the increase of foundation pit excavation depth, the maximum surface settlement increases continuously. The maximum settlement position of the west surface does not change with the change of excavation conditions (except the first excavation step). The maximum surface settlement is about 0.029% of the final excavation depth of the foundation pit and about 67% of the maximum horizontal displacement of the diaphragm wall. The maximum surface settlement is located 20 m away from the edge of the

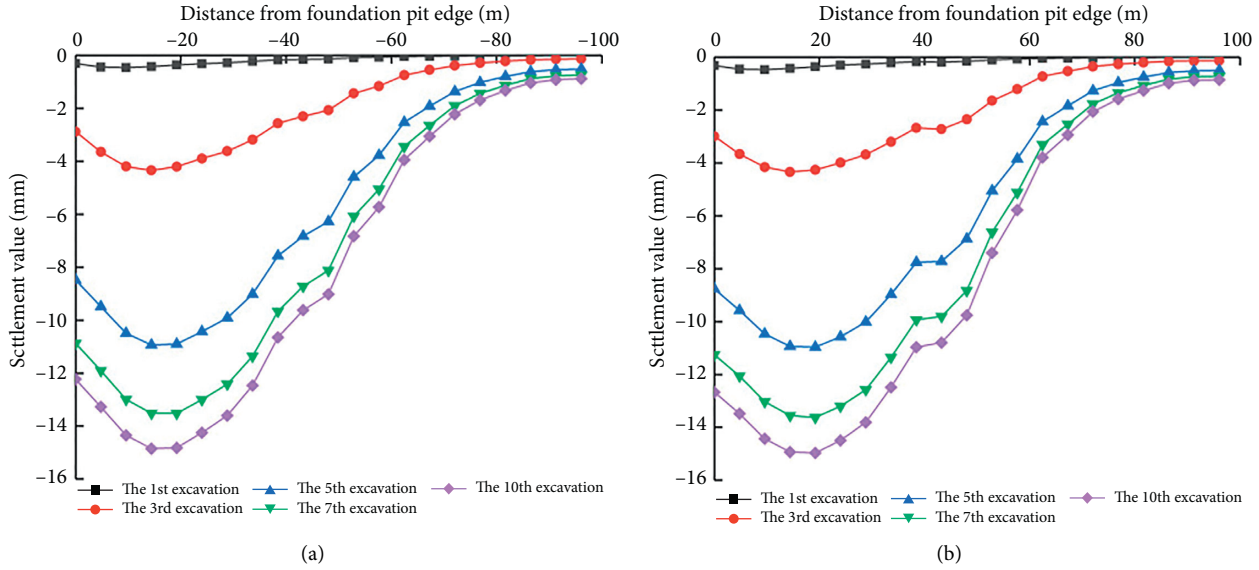

Figure 13: The curve of surface subsidence. (a) West wall. (b) East wall.

Table 6: Summary of the corresponding position of the maximum subsidence of the surface.

Working procedure	External surface of foundation pit (west)		External surface of foundation pit (east)	
	Maximum settlement (mm)	Distance from foundation pit edge (m)	Maximum settlement (mm)	Distance from foundation pit edge (m)
The first excavation step (−2.000 m)	−0.460	10.00	−0.470	10.00
The third excavation step (−13.400 m)	−4.340	15.00	−4.339	15.00
The fifth excavation step (−24.550 m)	−10.938	15.00	−10.968	20.00
The seventh excavation step (−34.145 m)	−13.515	15.00	−13.626	20.00
The tenth excavation step (−51.630 m)	−14.851	15.00	−14.967	20.00

foundation pit, about 0.4 times the final excavation depth of the foundation pit, and the main influence area is about 1.5 times the final excavation depth of the foundation pit.

4.2. Numerical Simulation Study on Construction Effect of Top-Down Construction Method for Foundation Pit with Suspended Foot Diaphragm Wall

4.2.1. Research Background of Optimization of Suspended Diaphragm Wall. In the original design scheme of the Jiangbei working shaft foundation pit, the height of the diaphragm wall is 59.8 m, the thickness is 1.5 m, and the bottom of the diaphragm wall is at the same elevation. However, in the construction process, due to the high strength of moderately weathered rock, the construction speed of existing wall forming equipment is too slow to meet the requirements of the construction period, and the cost is too high. Through the discussion of experts, it is proposed to change the insertion mode of in situ diaphragm wall into the design scheme of a suspended foot diaphragm wall with two meters into the rock. The length of the left wall (west wall) of the suspended foot diaphragm wall is 45.82 m, and the length of the right wall (east wall) is 51.98 m, as shown in Figure 14. Other conditions are completely consistent with the same length diaphragm wall in Section 4.1.

Therefore, the purpose of numerical simulation under this condition is to study the deformation law of the suspended diaphragm wall foundation pit during top-down construction. Through the theoretical analysis of the data obtained from the numerical simulation, the purpose of optimizing the diaphragm wall can be achieved. The data and analysis results can be used as reference materials for related projects.

4.2.2. Analysis of Simulation Results of Horizontal Displacement of Suspended Diaphragm Wall (The Depth into Rock is 2 m). Here, it should be emphasized that since the horizontal displacement, bending moment, and surface settlement contour plot obtained by the simulation of the construction effect of the suspended diaphragm wall are similar to those of the diaphragm wall with the same length,

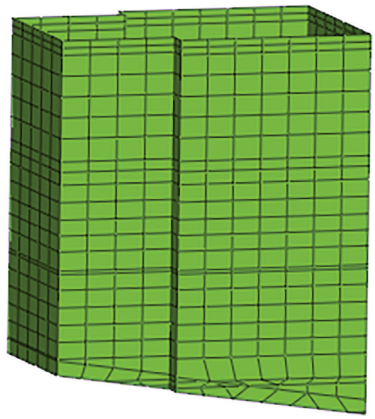

Figure 14: Schematic diagram of the ground connection wall (the depth into the rock is 2 m).

the simulation contour plot corresponding to the above three construction effect indexes is no longer displayed here.

The data of the horizontal displacement of the diaphragm wall under five simulated excavation conditions are sorted out and analyzed, and the depth-displacement curve of the diaphragm wall is obtained, as shown in Figure 15, and the maximum horizontal displacement and depth data of the diaphragm wall are summarized into a table, as shown in Table 7.

It can be seen from the above that the horizontal displacement of the foot diaphragm wall is small in the first excavation step. With the excavation of the foundation pit, the pouring of the middle plate structure, and the support of the ring frame beam, the horizontal displacement curve of the foot diaphragm wall is in the shape of "small at both ends, large in the middle." When the diaphragm wall is a suspended footing and the underlying strata are less embedded, the displacement and deformation of the end and bottom of the suspended footing diaphragm wall are larger. The maximum horizontal displacement of the east wall is greater than that of the west wall, which is due to the existence of the inclined rock surface. The displacement and deformation of the east and west walls are asymmetric. The maximum horizontal displacement of the diaphragm wall gradually moves down with the increase of the excavation depth and finally above the excavation surface. The maximum horizontal displacement is about 7/10 ~3/4 times the final excavation depth of the foundation pit.

4.2.3. Analysis of Bending Moment Simulation Results of Suspended Diaphragm Wall (The Depth into Rock Is 2 m). By sorting and analyzing the data in the bending moment cloud part of the suspended footed diaphragm wall under five simulated excavation step conditions, the relationship curve between depth and bending moment of the suspended footed diaphragm wall can be obtained, as shown in Figure 16, and the maximum bending moment and depth data of the suspended footed diaphragm wall can be summarized into a table, as shown in Table 8.

It can be seen from the above that the bending moment of the diaphragm wall is small in the first excavation step, and there is a reverse bending point. With the progress of excavation, the bending moment of the diaphragm wall increases gradually and then decreases slightly in the final excavation stage. The maximum positive moment is larger than the maximum negative moment at each excavation stage. The position of the maximum positive bending moment of the east and west walls first moves down and then rises and then remains unchanged after the original position. The position of the maximum negative bending moment does not change with the change of the excavation stage (except for the tenth excavation of the east wall). Due to the existence of inclined strata, the maximum bending moment of the east wall is larger than that of the west wall in each excavation stage (except for the negative bending moment of the tenth excavation step), and the deformation law of the east wall and the west wall is basically the same, but asymmetric. In each excavation stage, the maximum positive bending moment of the diaphragm wall is larger than the maximum negative bending moment. The maximum positive bending moment of the diaphragm wall is about 7/10~3/4 times the final excavation depth of the foundation pit, and the maximum negative bending moment is about 4/5~19/20 times the final excavation depth of the foundation pit.

4.2.4. Analysis of Simulation Results of Ground Settlement of Suspended Diaphragm Wall (The Depth into Rock Is 2 m). By sorting and analyzing the simulated data of soil surface settlement under five excavation step conditions, the surface settlement distance curve from the foundation pit can be obtained, as shown in Figure 17, and the data of the location of the maximum surface settlement can be summarized into a table, as shown in Table 9.

It can be seen from the above that the settlement of soil surface is small at the first excavation step and increases gradually with the increase of excavation depth. In each construction stage, the surface settlement curve of soil increases first, then decreases, and finally tends to be stable with the distance from the foundation pit edge, showing a "groove" curve, and the surface settlement deformation law of the east and west sides is basically the same. The maximum settlement of the east and west sides of the ground is the same, and the final settlement is 0.3 times the final excavation depth of the foundation pit. The maximum surface settlement is about 0.036% of the final excavation depth of the foundation pit, about 78% of the maximum horizontal displacement of the foot diaphragm wall. The maximum surface settlement is located at a distance of 15 m from the edge of the foundation pit, about 0.3 times the final excavation depth of the foundation pit, and the main impact area is about 1.5 times the final excavation depth of the foundation pit.

4.3. Comparative Analysis of Simulation Results under Two Conditions

4.3.1. Comparative Analysis of Horizontal Displacement of the Diaphragm Wall. After sorting and analyzing the data in

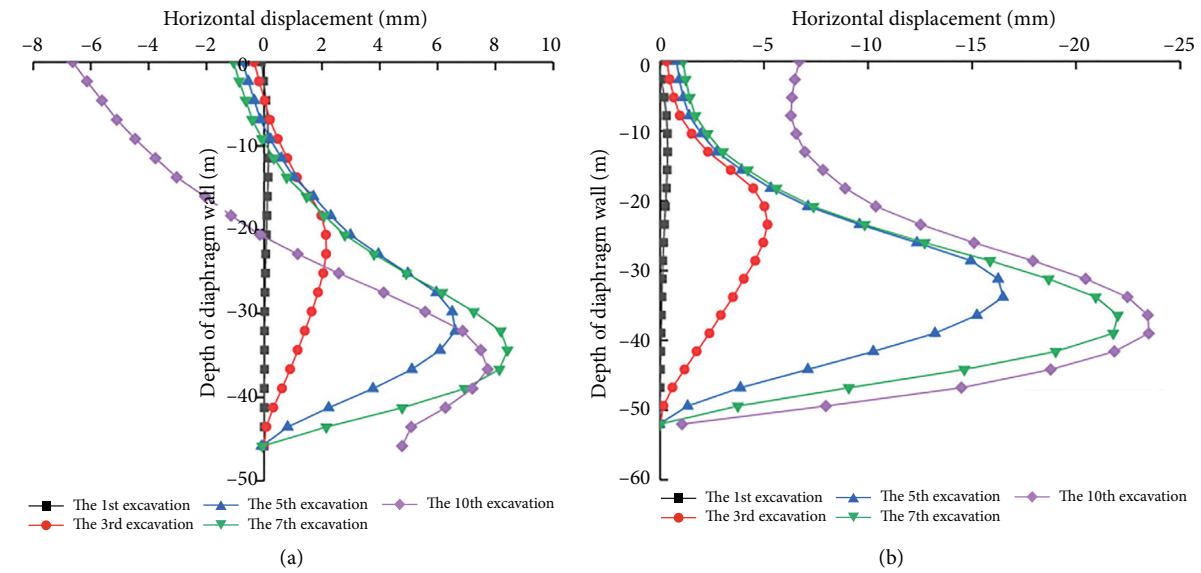

Figure 15: The horizontal displacement curve of the suspended foot diaphragm wall. (a) West wall. (b) East wall.

Table 7: Summary table of the corresponding depth of the maximum horizontal displacement of the suspended foot diaphragm wall.

Working procedure	Suspended foot diaphragm wall (west, the length is 45.82 m)		Suspended foot diaphragm wall (east, the length is 51.98 m)	
	Maximum horizontal displacement (mm)	The depth of the diaphragm wall (m)	Maximum horizontal displacement (mm)	The depth of the diaphragm wall (m)
The first excavation step (−2.000 m)	0.141	−11.46	−0.371	−13.00
The third excavation step (−13.400 m)	2.146	−22.91	−5.170	−23.39
The fifth excavation step (−24.550 m)	6.613	−32.07	−16.490	−33.79
The seventh excavation step (−34.145 m)	8.418	−34.37	−22.006	−36.39
The first excavation step (−2.000 m)	7.738	−36.66	−23.497	−38.99

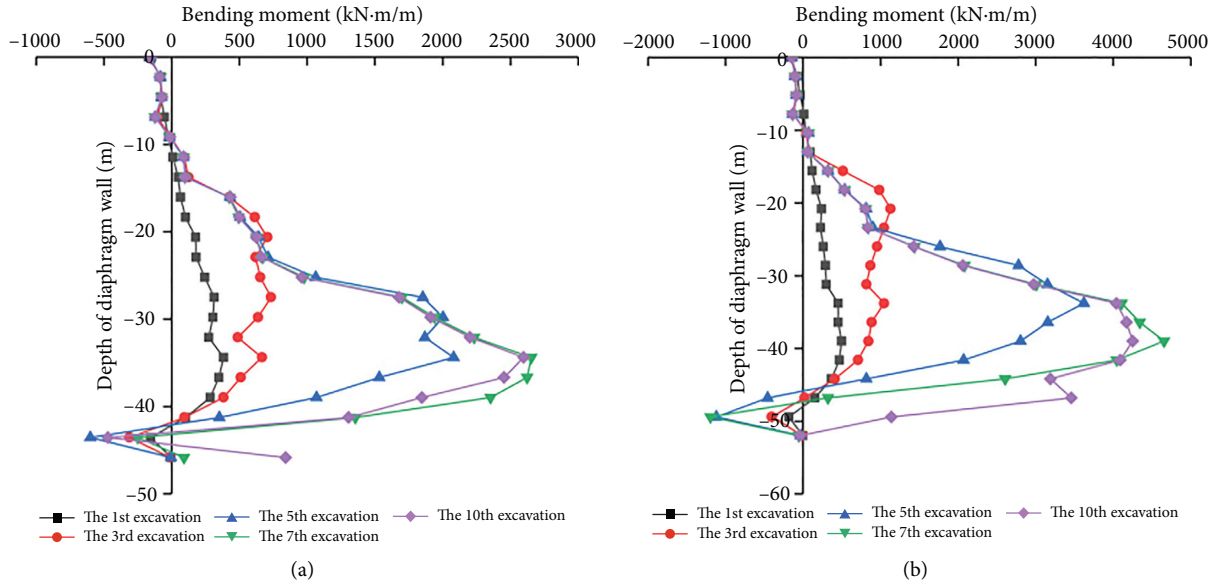

Figure 16: The bending moment curve of the suspended foot diaphragm wall. (a) West wall. (b) East wall.

Table 8: Summary of the corresponding depth of the maximum bending moment of the suspended foot connecting wall.

Working procedure	Suspended foot diaphragm wall (west, the length is 45.82 m)		Suspended foot diaphragm wall (east, the length is 51.98 m)	
	Maximum bending moment (kN·m/m)	The depth of the diaphragm wall (m)	Maximum bending moment (kN·m/m)	The depth of the diaphragm wall (m)
The first excavation step (−2.000 m)	383.553/−154.641	−34.37/−43.53	495.496/−183.378	−38.99/−49.38
The third excavation step (−13.400 m)	732.862/−311.066	−27.49/−43.53	1127.781/−404.225	−20.79/−49.38
The fifth excavation step (−24.550 m)	2080.852/−600.905	−34.37/−43.53	3621.628/−1118.857	−33.79/−49.38
The seventh excavation step (−34.145 m)	2654.072/−250.395	−34.37/−43.53	4654.927/−1193.643	−38.99/−49.38
The first excavation step (−2.000 m)	2596.608/−469.726	−34.37/−43.53	4251.651/−42.949	−38.99/−51.98
Remarks	Among the maximum bending moments in the table, the maximum positive bending moment value is before "/," and the maximum negative bending moment value is after "/," respectively, corresponding to the depth of the diaphragm wall			

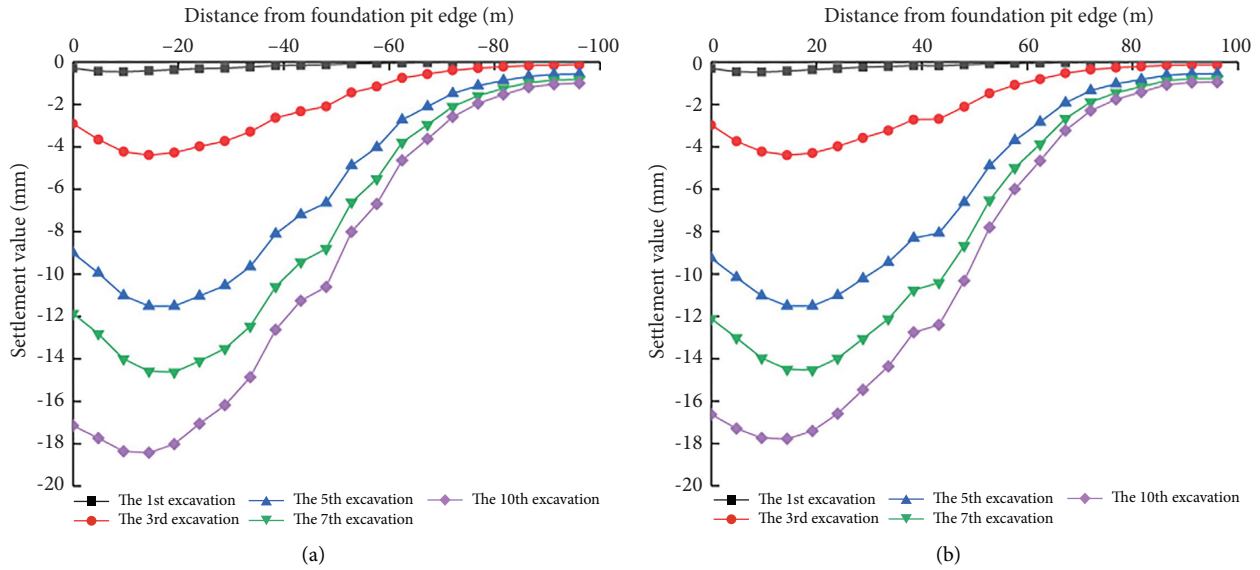

Figure 17: The curve of the surface settlement of the suspended foot diaphragm wall. (a) West wall. (b) East wall.

Table 9: Summary of the corresponding position of the maximum subsidence of the surface.

Working procedure	External surface of foundation pit (west)		External surface of foundation pit (east)	
	Maximum settlement (mm)	Distance from foundation pit edge (m)	Maximum settlement (mm)	Distance from foundation pit edge (m)
The first excavation step (−2.000 m)	−0.459	10.00	−0.476	10.00
The third excavation step (−13.400 m)	−4.385	15.00	−4.393	15.00
The fifth excavation step (−24.550 m)	−11.511	20.00	−11.511	20.00
The seventh excavation step (−34.145 m)	−14.621	20.00	−14.526	20.00
The tenth excavation step (−51.630 m)	−18.419	15.00	−17.778	15.00

the contour plot of horizontal displacement of diaphragm wall during the 10th excavation step (that is, the foundation pit is excavated to the bottom) under two working conditions, the depth-displacement curve of the diaphragm wall under two working conditions can be obtained, as shown in Figure 18, and the maximum horizontal displacement and depth data of diaphragm wall under two working conditions can be summarized into a table, as shown in Table 10.

The following can be seen from Figure 18 and Table 10:

(1) In the tenth excavation step, it entered the moderately weathered rock with high strength. In case 1, the maximum horizontal displacement of the west wall is 8.256 mm, which is at the depth of −32.89 m. The maximum horizontal displacement of the east wall is −22.341 mm, which is located at the depth of −38.87 m. In case 2, the maximum horizontal displacement of the west wall is 7.738 mm at the depth of −36.66 m. The maximum horizontal displacement of the east wall is −23.497 mm, which is located at the depth of −38.99 m.

(2) From the comparison of the two working conditions, it can be seen that the maximum horizontal displacement of the west wall is reduced by 0.518 mm, the maximum horizontal displacement of the east wall is increased by 1.156 mm, the horizontal displacement of the end and bottom of the diaphragm wall is increased suddenly, and the stability of the diaphragm wall is poor, which is due to the large horizontal displacement and deformation due to the lack of rock embedment in working condition 2. Therefore, the horizontal displacement of condition 2 is larger than that of condition 1, and the maximum horizontal displacement of condition 2 moves down.

4.3.2. Bending Moment Analysis of Diaphragm. By sorting and analyzing the data in the bending moment cloud part of the diaphragm wall during the 10th excavation step (i.e., the foundation pit is excavated to the bottom) under two working conditions, the depth-bending moment curve of the diaphragm wall under two working conditions can be obtained, as shown in Figure 19, and the maximum bending moment and depth data of diaphragm wall under two working conditions can be summarized into a table, as shown in Table 11.

The following can be seen from Figure 19 and Table 11:

(1) In the tenth excavation step, it enters the moderately weathered rock stratum with high strength on the left and low strength on the right. In case 1, the maximum positive bending moment of the west wall is 2462.475 kN·m/m, which is located at the depth of −35.88 m. The maximum positive bending moment of the east wall is 4271.144 kN·m/m, which is located at the depth of −38.87 m. The maximum negative bending moment of the west wall is −838.087 kN·m/m, which is located at the depth of −44.85 m. The maximum negative bending moment of the east wall is −3594.525 kN·m/m, which is located at the depth of −50.83 m. In case 2, the maximum positive bending moment of the west wall is 2596.608 kN·m/m, which is located at the depth of −34.37 m. The maximum positive bending moment of the east wall is 4251.651 kN·m/m, which is located at the depth of −38.99 m. The maximum negative bending moment of the west wall is −469.726 kN·m/m, which is located at the depth of −43.53 m. The maximum negative bending moment of the east wall is −42.949 kN·m/m, which is located at the depth of −51.98 m.

(2) From the comparison of the two working conditions, it can be seen that the maximum positive bending moment of the east wall and the west wall increases, and the maximum negative bending moment decreases sharply in case 2 compared with case 1. There is a large positive bending moment at the bottom of the west wall and a small negative bending moment at the bottom of the east wall. This is because when the foot diaphragm wall is excavated to the bottom of the foundation pit, the west wall has no embedded restraint effect of the rock layer, and the east wall is embedded in the rock layer very shallow. In case 2, the maximum positive (negative) bending moment of the west wall moves up slightly, the maximum positive (negative) bending moment of the east wall moves down slightly, and the maximum negative bending moment of the east wall is located at the bottom of the diaphragm wall. In both cases, the maximum positive bending moment of the east and west walls appears above the excavation face, which indicates that the rock embedment in the diaphragm wall has a great constraint on the bending moment deformation of the diaphragm wall. The maximum positive moment of the two walls is larger than the maximum negative moment. Because of the existence of inclined rock, the maximum bending moment of the east wall is larger than that of the west wall.

4.3.3. Comparative Analysis of Ground Settlement of Diaphragm Wall. By sorting and analyzing the data in the contour plot of ground settlement of diaphragm wall soil mass during the 10th excavation step (i.e., excavation to the bottom) under two working conditions, the curve of ground settlement distance from the edge of the foundation pit under two working conditions can be obtained, as shown in Figure 20, and the data of maximum ground settlement position under two working conditions can be summarized into a table, as shown in Table 12.

The following can be seen from Figure 20 and Table 12:

(1) The tenth excavation step, into the moderately weathered rock. In case 1, the maximum settlement of the soil surface on the west side of the foundation pit is −14.851 mm, which is 15 m away from the side of the foundation pit. The maximum surface settlement of the east side soil is −14.967 mm, which is

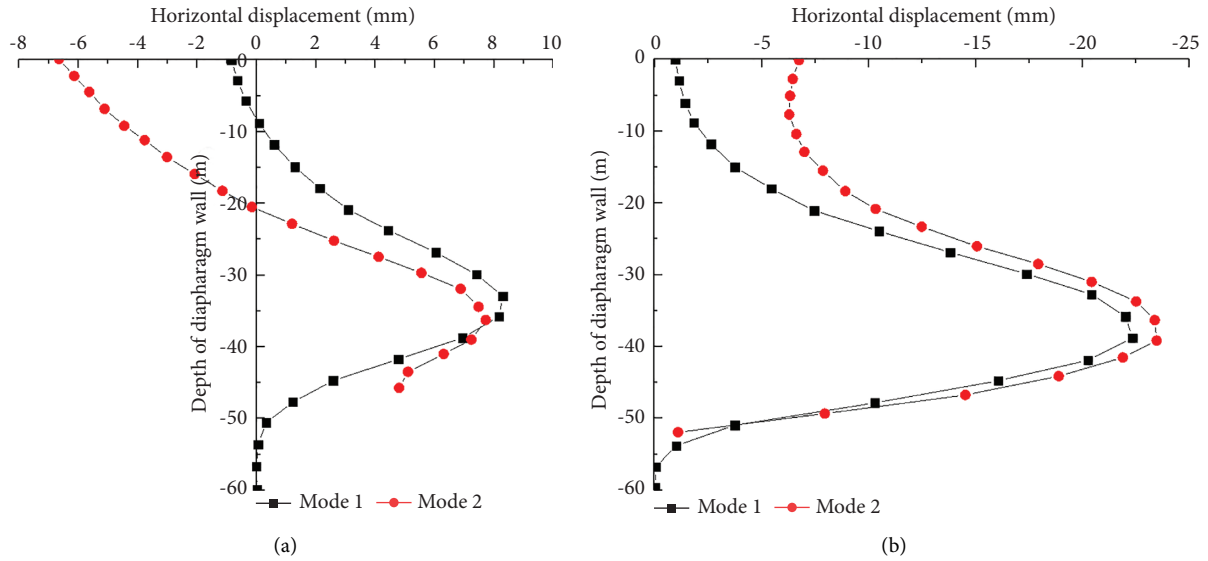

Figure 18: The horizontal displacement curve of the diaphragm wall. (a) West wall. (b) East wall.

Table 10: The corresponding depth of maximum horizontal displacement of diaphragm wall during the 10th excavation step under two working conditions.

Working procedure	Diaphragm wall (west)		Diaphragm wall (east)	
	Maximum horizontal displacement (mm)	The depth of the diaphragm wall (m)	Maximum horizontal displacement (mm)	The depth of the diaphragm wall (m)
Diaphragm wall of the same length (working condition 1)	8.256	−32.89	−22.341	−38.87
Suspended foot diaphragm wall (working condition 2)	7.738	−36.66	−23.497	−38.99

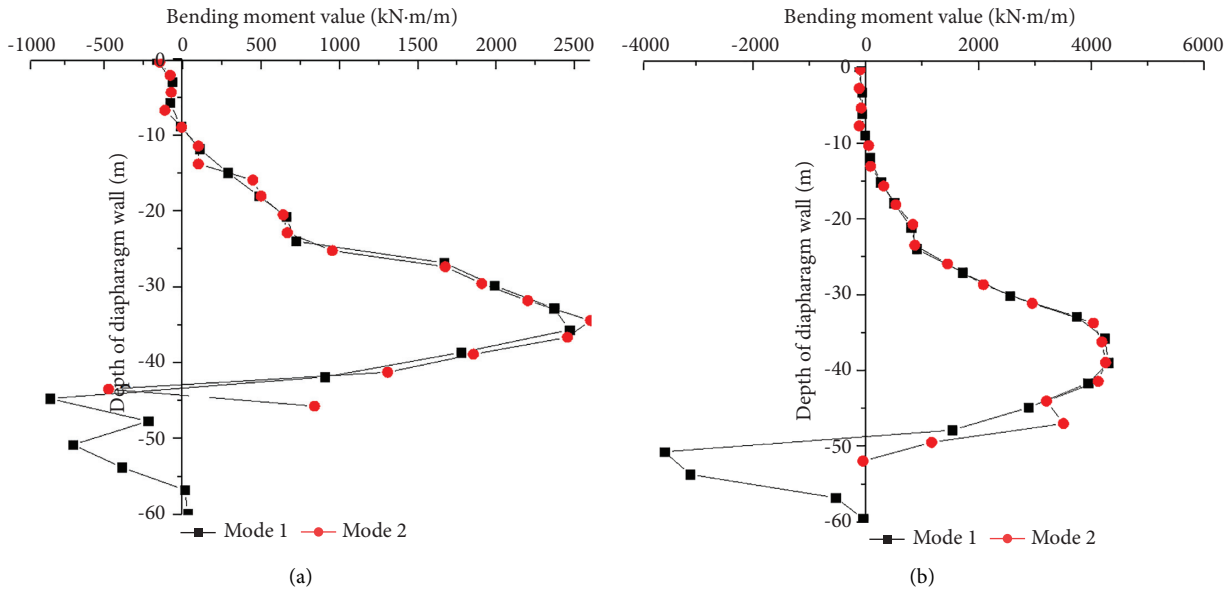

Figure 19: Bending moment diagram of the diaphragm wall. (a) West wall. (b) East wall.

Table 11: The corresponding depth of maximum bending moment of diaphragm wall in the 10th excavation step under two working conditions.

Working procedure	Diaphragm wall (west)		Diaphragm wall (east)	
	Maximum bending moment (kN·m/m)	The depth of the diaphragm wall (m)	Maximum bending moment (kN·m/m)	The depth of the diaphragm wall (m)
Diaphragm wall of the same length (working condition 1)	2462.475/−838.087	−35.88/−44.85	4271.144/−3594.525	−38.87/−50.83
Suspended foot diaphragm wall (working condition 2)	2596.608/−469.726	−34.37/−43.53	4251.651/−42.949	−38.99/−51.98

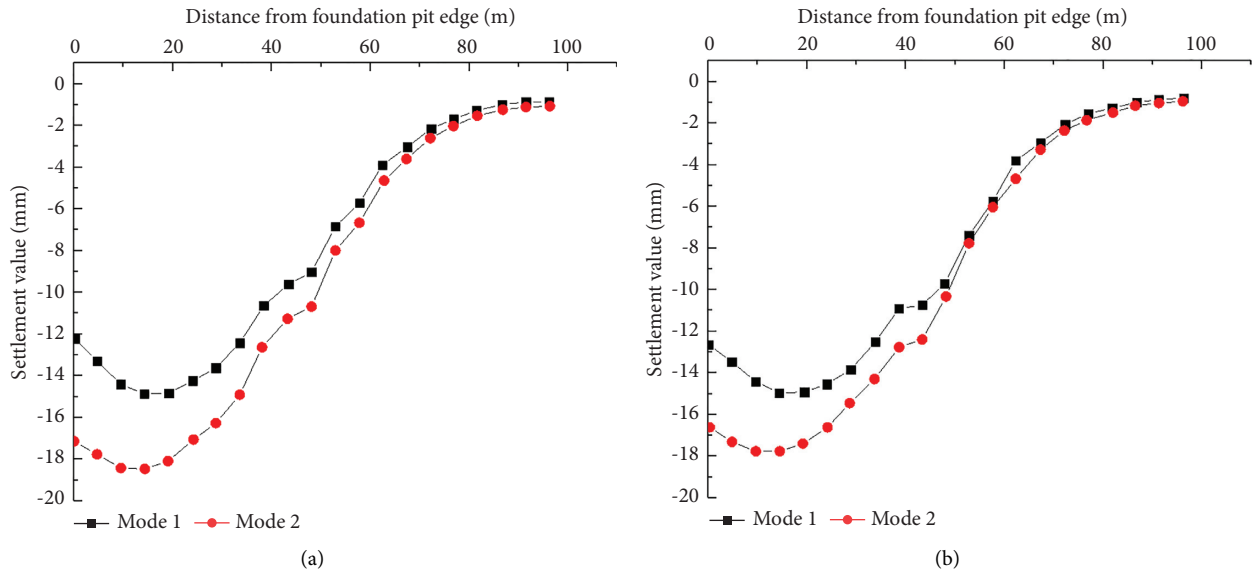

Figure 20: The curve of surface subsidence. (a) West wall. (b) East wall.

Table 12: Summary of corresponding positions of maximum ground settlement during the 10th excavation step under two working conditions.

Working procedure	External surface of foundation pit (west)		External surface of foundation pit (east)	
	Maximum settlement (mm)	Distance from foundation pit edge (m)	Maximum settlement (mm)	Distance from foundation pit edge (m)
Diaphragm wall of the same length (working condition 1)	−14.851	15.00	−14.967	20.00
Suspended foot diaphragm wall (working condition 2)	−18.419	15.00	−17.778	15.00

20 m away from the side of the foundation pit. In case 2, the maximum settlement of the soil surface on the west side of the foundation pit is −18.419 mm, which is 15 m away from the side of the foundation pit. The maximum surface settlement of the east side soil is −17.778 mm, which is 15 m away from the side of the foundation pit.

(2) From the comparison of the two conditions, it can be seen that compared with condition 1, the maximum settlement of soil surface in condition 2 increases by 2.5~3.5 mm, which is because the rock has a little constraint on the foot diaphragm wall. The maximum settlement position of the soil surface on the west side remains unchanged, and the maximum settlement position of the soil surface on the east side moves to 15 m away from the edge of the foundation pit. With the distance from the foundation pit edge, the surface settlement curve of soil under the two conditions first increases, then decreases, and finally tends to be stable, showing a "groove" curve, and the surface settlement deformation law of the east and west sides is basically the same.

5. Field Measurement Verification

The top-down construction method of hanging footed diaphragm wall foundation pit is adopted. The surface settlement of the diaphragm wall, deep horizontal displacement

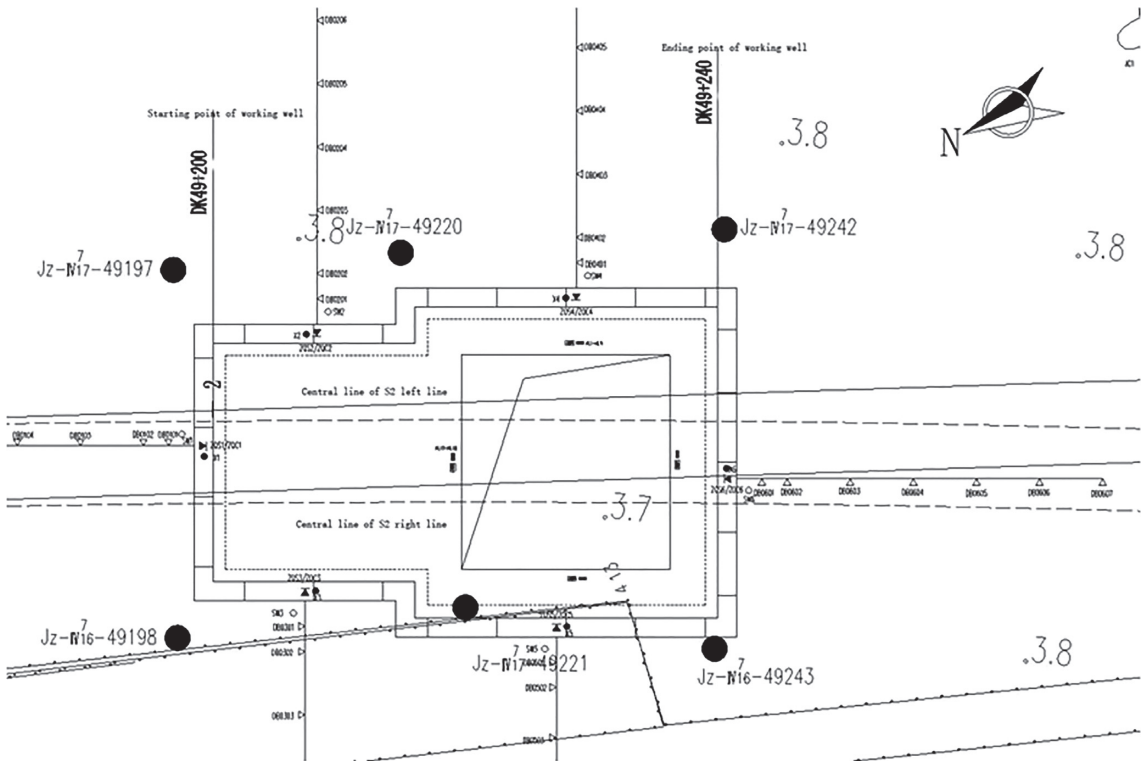

Figure 21: Layout of monitoring points.

Table 13: Measuring point information.

Monitoring content	Measuring point ID	Number of measuring points
Ground settlement of diaphragm wall	DBC-1-1~DBC-1-4 DBC-2-1~DBC-2-6 DBC-3-1~DBC-3-4 DBC-4-1~DBC-4-5 DBC-5-1~DBC-5-4 DBC-6-1~DBC-6-7	30
Deep horizontal displacement of diaphragm wall	CXQ1~CXQ6	6
Axial force of concrete support	ZCL1-1~ZCL1-4 ZCL2-1~ZCL2-4 ZCL3-1~ZCL3-4 ZCL4-1~ZCL4-4 ZCL5-1~ZCL5-4 ZCL6-1~ZCL6-4 ZCL7-1~ZCL7-4 ZCL8-1~ZCL8-4	32

of wall, and axial force of concrete support are monitored at the construction site. The layout of monitoring points is shown in Figure 21, and the label information of measuring points is shown in Table 13.

The cumulative deformation curve of surface settlement is shown in Figure 22, the variation curve of concrete support axial force is shown in Figure 23, and the variation curve of deep horizontal displacement of diaphragm wall is shown in Figure 24.

Through the analysis of the variation curve of the field measured data from Figures 22 to Figure 24 and the comparison with the above numerical simulation results, although there are differences in values, they are all within the acceptable range, which verifies the correctness of the

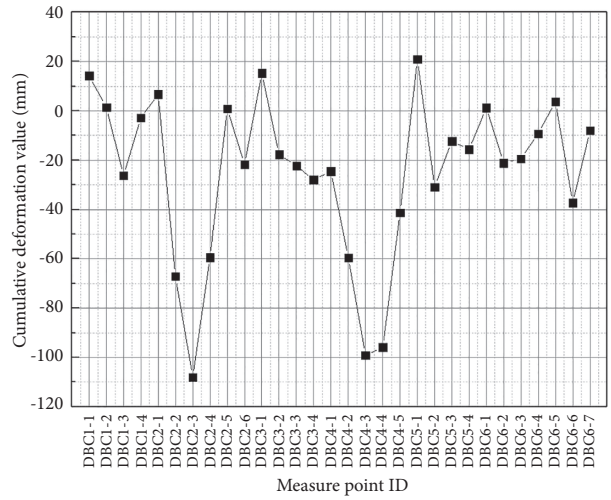

Figure 22: Cumulative deformation of surface settlement.

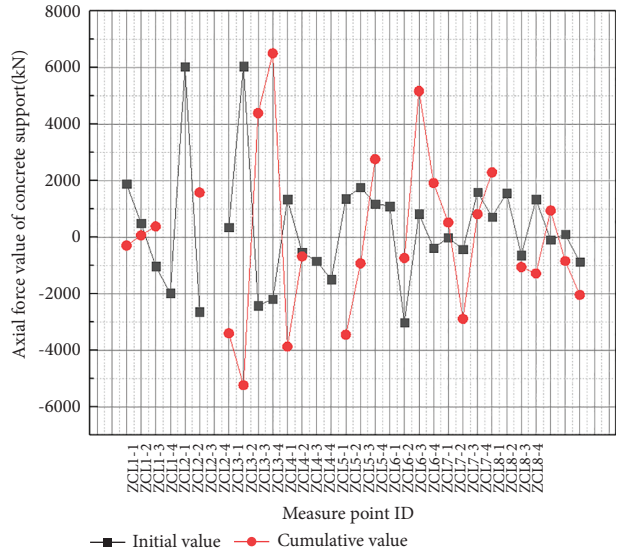

Figure 23: Variation curve of axial force of concrete support.

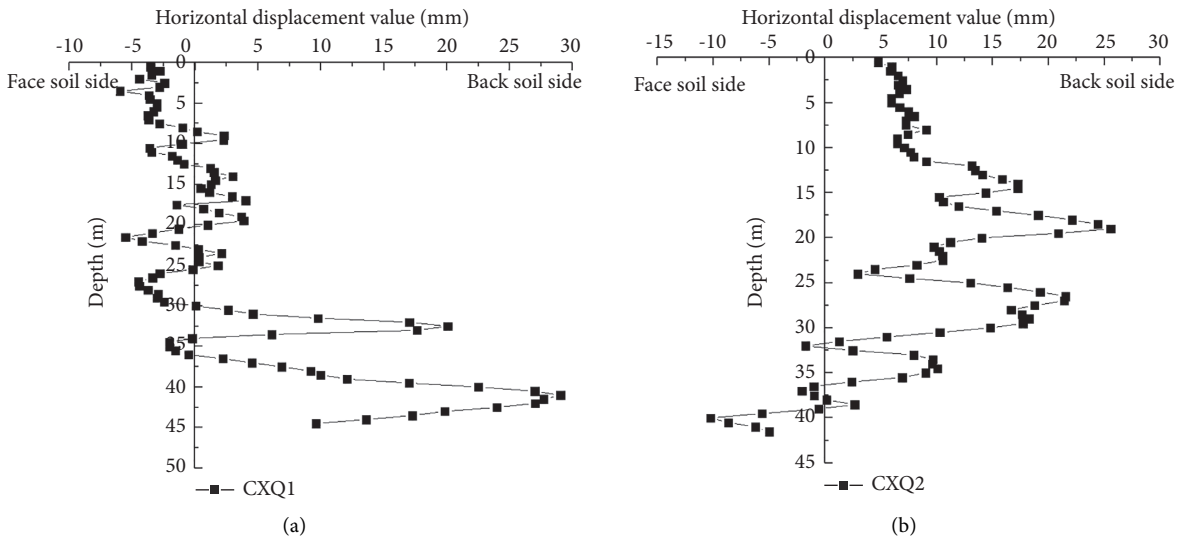

Figure 24: Continued.

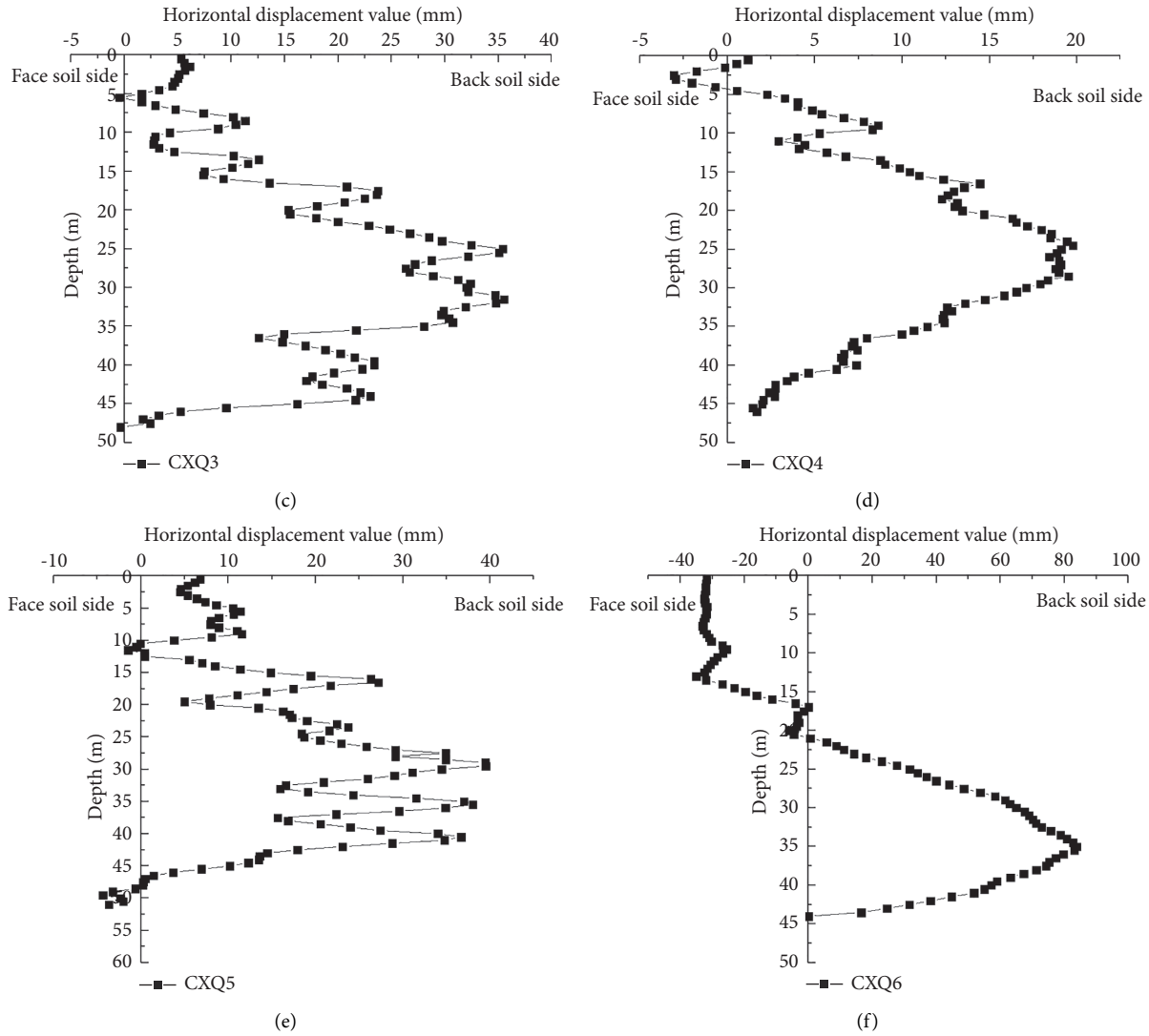

Figure 24: Variation curve of deep horizontal displacement of the diaphragm wall.

numerical simulation results and the reliability of the top-down construction of the foundation pit with suspended feet and ground walls.

6. Conclusion

In this paper, the construction effect of the top-down construction method for the diaphragm wall of foundation pit under two working conditions of diaphragm wall with the same length and suspended foot is simulated, and the horizontal displacement, bending moment, and surface settlement deformation law of diaphragm wall of foundation pit are analyzed.

(1) When the foundation pit with the same length is excavated by the top-down construction method, the horizontal displacement of the diaphragm wall is small at the first excavation. With the excavation of the foundation pit, the deformation law of "small at both ends and large in the middle" is formed as a whole of the horizontal displacement curve of the diaphragm wall. The position of the maximum horizontal displacement of the diaphragm wall gradually moves down with the increase of the excavation depth, which is 3/5~3/4 times the final excavation depth of the foundation pit, while the position of the maximum positive and negative bending moments of the diaphragm wall is close to the bottom of the foundation pit. The surface settlement of soil is very small during the first excavation step, and it is in "groove shape" with the gradual increase of excavation. The maximum surface settlement is smaller than the excavation depth and the maximum horizontal displacement of the diaphragm wall. This value occurs at a distance of 20 m from the edge of the foundation pit, and the main influence area is about 1.5 times the final excavation depth of the foundation pit.

(2) When the foundation pit of the hanging foot ground connecting wall is excavated by reverse method, The horizontal displacement curve of the hanging foot ground connecting wall is in the shape of "small at both ends and large in the middle." The maximum horizontal displacement position of the diaphragm wall gradually moves down with the increase of excavation depth, which is about 7/10~3/4 of the final excavation depth. In each excavation stage, the maximum positive bending moment of the diaphragm wall is greater than the maximum negative bending moment. The maximum positive and negative bending moments of the diaphragm wall are close to the bottom of the foundation pit. The maximum surface settlement is about 0.036% of the final excavation depth of the foundation pit, about 78% of the maximum horizontal displacement of the hanging foot ground connecting wall, which is 15 m away from the edge of the foundation pit, and the main influence area is about 1.5 times of the final excavation depth. The horizontal displacement, bending moment, and surface settlement of the suspended foot diaphragm wall decrease with the increase of the depth of the suspended foot diaphragm wall into the rock. However, the greater the depth into the rock, the better it becomes. When the depth of the rock increases to a certain extent, the role of continuously increasing the depth of the rock is no longer obvious. Therefore, in the actual project, the appropriate depth into the rock is selected on the premise of ensuring the safety of the foundation pit and reducing the cost.

Therefore, through the comparative analysis of the simulation results, it can be seen that compared with the top-down construction method of the same length diaphragm wall, the simulation results of the top-down construction method of the suspended foot diaphragm wall foundation pit are relatively better. At the same time, combined with the general situation of relying on the project and the suggestions given by experts, it is more suitable to use the suspended foot diaphragm wall for the construction of the foundation pit diaphragm wall.

(3) Through the comparative analysis of the field monitoring data and the simulation results, the correctness of the numerical simulation results is verified, and the reliability of the reverse construction method of the hanging foot ground wall foundation pit is also verified.

Data Availability

The data used to support the findings of this study are available from the corresponding author upon request.

Conflicts of Interest

The authors declare that they have no conflicts of interest.

Acknowledgments

This work was supported by the Wenzhou Railway and Rail Transit Investment Co., Ltd, and Shanghai Tunnel Engineering Co., Ltd.

References

[1] N. Benmebarek, S. Benmebarek, R. Kastner, and A.-H. Soubra, "Passive and active earth pressures in the presence of groundwater flow," *Géotechnique*, vol. 56, no. 3, pp. 149–158, 2006.

[2] G. Zheng and Y. Jiao, *Design Theory and Engineering Application of Deep Foundation Pit*, China Construction Industry Press, China, Chinese, 2010.

[3] X. Yang, "Application and development of new technology for deep foundation pit support in soft soil foundation along the coast of Zhejiang," *Journal of Geotechnical Engineering*, vol. 2012, no. S1, p. 7, 2012, in Chinese.

[4] X. Wang, "Analysis of deformation of retaining wall of deep foundation pit works in podium of Shanghai Center Tower," *Chinese Journal of Rock Mechanics and Engineering*, vol. 2, pp. 421–431, 2012, in Chinese.

[5] I. H. Wong, T. Y. Poh, and H. L. Chuah, "Performance of excavations for depressed expressway in Singapore," *Journal of Geotechnical and Geoenvironmental Engineering*, vol. 123, no. 7, pp. 617–625, 1997.

[6] K. Mccue and D. Clark, "Australian paleoseismology: towards a better basis for seismic hazard estimation," *Annals of Geophysics*, vol. 46, no. 5, 2003.

[7] Y. D. Wu, J. Liu, and C. W. W. Ng, "Effects of pile extraction and refilling with cement slurry on ground settlements," *Canadian Geotechnical Journal*, vol. 50, no. 3, pp. 343–349, 2013.

[8] J. W. Hong, H. E. Wei, and Y. I. Li-Yun, "Hand-dug hole pile foundation reinforcement by high-pressure grouting sodium silitcae cement slurry," *Technology & Economy in Areas of Communications*, 2015.

[9] H. B. Zhang, J. J. Chen, X. S. Zhao, J.-H. Wang, and H. Hu, "Displacement performance and simple prediction for deep excavations supported by contiguous bored pile walls in soft clay," *Journal of Aerospace Engineering*, vol. 28, no. 6, pp. A4014008.1–A4014008.10, 2015.

[10] P.-G. Hsieh and C.-Y. Ou, "Simplified approach to estimate the maximum wall deflection for deep excavations with cross walls in clay under the undrained condition," *Acta Geotechnica: An International Journal for Geoengineering*, vol. 11, no. 1, pp. 177–189, 2016.

[11] P.-G. Hsieh and C.-Y. Ou, "Shape of ground surface settlement profiles caused by excavation," *Canadian Geotechnical Journal*, vol. 35, no. 6, pp. 1004–1017, 1998.

[12] C. Yoo and D. Lee, "Deep excavation-induced ground surface movement characteristics—a numerical investigation," *Computers and Geotechnics*, vol. 35, no. 2, pp. 231–252, 2008.

[13] S. K. Bose and N. N. Som, "Parametric study of a braced cut by finite element method," *Computers and Geotechnics*, vol. 22, no. 2, pp. 91–107, 1998.

[14] C. W. Ng, B. Simpson, M. L. Lings, and D. Nash, "Numerical analysis of a multipropped excavation in stiff clay," *Canadian Geotechnical Journal*, vol. 35, no. 1, pp. 115–130, 1998.

[15] R. J. Finno, D. K. Atmatzidis, and S. B. Perkins, "Observed performance of a deep excavation in clay," *Journal of Geotechnical Engineering*, vol. 115, no. 8, pp. 1045–1064, 2016.

[16] H. G. Poulos, "Analysis of the settlement of pile groups," *Géotechnique*, vol. 18, no. 4, pp. 449–471, 1968.
[17] M. D. Bolton and W. Powrie, "Behaviour of diaphragm walls in clay prior to collapse," *Géotechnique*, vol. 38, no. 2, pp. 167–189, 1988.
[18] C.-Y. Ou, J.-T. Liao, and H.-D. Lin, "Performance of diaphragm wall constructed using top-down method," *Journal of Geotechnical and Geoenvironmental Engineering*, vol. 124, no. 9, pp. 798–808, 1998.
[19] J. Graham, "The 2003 R.M. Hardy Lecture: soil parameters for numerical analysis in clay," *Canadian Geotechnical Journal*, vol. 43, no. 2, pp. 187–209, 2006.
[20] J. Wang, Z. Xu, and J. Chen, "Etc Analysis on deformation characteristics of diaphragm wall of deep foundation pit in soft soil area of Shanghai," *Journal of Underground Space and Engineering*, vol. 1, no. 4, pp. 485–489, 2005, in Chinese.
[21] Z Xu, J Wang, and W Wang, "Deformation behavior of diaphragm wall in deep foundation pit engineering in Shanghai," *Journal of Civil Engineering*, vol. 41, no. 8, pp. 81–86, 2008, in Chinese.
[22] J. Qiu, A. Shi, and Y. Xia, "Etc Three dimensional finite element analysis of spatial deformation of double row lattice diaphragm wall," *Water Resources and Hydropower Technology*, vol. 45, no. 8, pp. 78–82, 2014, in Chinese.
[23] S He, G Wu, and Z Zhu, "Finite element analysis of influencing factors of deep foundation pit support design," *Journal of Rock Mechanics and Engineering*, vol. S22005, in Chinese.